Published for SISSA by Springer

Received: February 7, 2012
Revised: May 5, 2012
Accepted: June 7, 2012
Published: June 22, 2012

Mimicking the standard model Higgs boson in UMSSM

Chun-Fu Chang,[a] **Kingman Cheung,**[a,b] **Yi-Chuen Lin**[a] **and Tzu-Chiang Yuan**[c]

[a] *Department of Physics, National Tsing Hua University, Hsinchu 300, Taiwan*
[b] *Division of Quantum Phases & Devices, School of Physics, Konkuk University, Seoul 143-701, Republic of Korea*
[c] *Institute of Physics, Academia Sinica, Nankang, Taipei 11529, Taiwan*

E-mail: electron0421@yahoo.com.tw, cheung@phys.nthu.edu.tw, yclin137@gmail.com, tcyuan@phys.sinica.edu.tw

Abstract: Motivated by the recent results in the standard model (SM) Higgs boson search at the Large Hadron Collider (LHC) we investigate the SM-like CP-even Higgs boson of the U(1)′-extended minimal supersymmetric standard model (UMSSM) and its branching ratio into the $b\bar{b}$, WW^*, and $\tilde{\chi}_1^0\tilde{\chi}_1^0$ modes. In the Summer 2011, a 2σ excess was reported in the channel $H \to WW^* \to \ell^+\nu\ell^-\bar{\nu}$ around $130-140\,\text{GeV}$ range. Later on in December 2011 announcements were made that an excess was seen in the $124-126\,\text{GeV}$ range, while the SM Higgs boson above 131 GeV up to about 600 GeV is ruled out. We examine two scenarios of these mass ranges: (i) $130\,\text{GeV} < M_{h_{\text{SM-like}}} < 141\,\text{GeV}$ and show that the Higgs boson can decay into invisible neutralinos to evade the SM bound; and (ii) $120\,\text{GeV} < M_{h_{\text{SM-like}}} < 130\,\text{GeV}$ and show that the Higgs boson can avoid decaying into neutralinos and thus gives enhanced rates into visible particles. We use the η model of E_6 with TeV scale supersymmetry to illustrate the idea by scanning the parameter space to realize these two different scenarios.

Keywords: Supersymmetry Phenomenology

ArXiv ePrint: 1202.0054

doi:10.1007/JHEP06(2012)128

JHEP06(2012)128

Contents

1 Introduction

The excitement of particle physics in the year 2011 was the hunt for the Higgs boson, the Higgs boson of any model, in particular that of the standard model (SM) at the Large Hadron Collider (LHC). The recent data in the Summer 2011 [1–5], showed an approximately 2σ excess in the channel $WW^* \to \ell^+\nu\ell^-\bar{\nu}$ ($\ell = e, \mu$) above the expected SM backgrounds. The excess is consistent with a Higgs boson of mass about 140 GeV but with a somewhat smaller production rate of $H \to WW^* \to \ell^+\nu\ell^-\bar{\nu}$ than the SM one. However, in December 2011 both ATLAS [6] and CMS [7] announced possible hints of excess in $\gamma\gamma$, WW, and ZZ channels that are consistent with a SM-like Higgs boson in the mass range of 124–126 GeV; and at the same time rule out a SM Higgs boson above 131 GeV up to about 600 GeV. Except for the $\gamma\gamma$ channel almost all channels are slightly suppressed relative to the SM cross sections at around 124–126 GeV. Note that these results consist of large errors. In this work, we consider two mass ranges, 120–130 and 130–141 GeV, for the SM-like Higgs boson of the U(1)′-extended minimal supersymmetric standard model (UMSSM). We will entertain these two ranges in the supersymmetry (SUSY) framework, because the current data are still premature to definitely confirm a Higgs boson, not to mention its mass.

Supersymmetric models in general predicts a light Higgs boson, mostly below about 150 GeV. In particular, the minimal supersymmetric standard model (MSSM) predicts

JHEP06(2012)128

a light Higgs boson with $M_h \lesssim 130\,\text{GeV}$. Thus, a Higgs boson heavier than 130 GeV significantly constrains the parameter space of the MSSM, forcing the sfermions masses to exceed the TeV range, and consequently SUSY loses somewhat of its appeal. It is then more natural to consider extensions to the MSSM if the light Higgs boson is heavier than 130 GeV, and to hide this Higgs boson by suppressing its branching ratio into visible modes. It is well known that by adding singlet Higgs field can easily raise the Higgs boson mass. Recent attempts to raise the Higgs boson mass in SUSY frameworks can be found in refs. [8–15], and attempts to hide such a light Higgs boson heavier than 130 GeV in the current data can be found in refs. [16–36].

On the other hand, if the SM-like Higgs boson falls in the mass range of 124–126 GeV and future data may further support that, this Higgs boson should decay into visible particles, almost in the same pattern as the SM Higgs boson, though the current data [6, 7] showed a slightly enhancement to the $\gamma\gamma$ mode while slightly suppression to the WW, ZZ, and $b\bar{b}$ modes. Recent attempts interpreting the 124–126 GeV Higgs boson in SUSY framework can be found in refs. [37–44]. In order to give a 124–126 GeV Higgs boson within MSSM, the stop sector must consist of a very heavy stop, a large mixing, and a relatively light stop, which has an interesting implication to collider phenomenology. However, within the MSSM it is rather difficult to enhance the $\gamma\gamma$ production rate but easier in some other extensions like the Randall-Sundrum scenario [45] and others [46–49].

It is therefore timely to investigate an extension of MSSM, which involves an extra $\text{U}(1)'$ symmetry and a Higgs singlet superfield S. The scalar component of the Higgs singlet superfield develops a vacuum expectation value (VEV), which breaks the $\text{U}(1)'$ symmetry and gives a mass to the $\text{U}(1)'$ gauge boson, denoted by Z'. At the same time, the VEV together with the Yukawa coupling can form an effective μ_{eff} parameter from the term $\lambda\langle S\rangle H_u H_d = \mu_{\text{eff}} H_u H_d$ in the superpotential, thus solving the μ problem of MSSM (the same as the NMSSM [50]).

Existence of extra neutral gauge bosons had been predicted in many extensions of the SM [51]. String-inspired models and grand-unification (GUT) models usually contain a number of extra U(1) symmetries, beyond the hypercharge $\text{U}(1)_Y$ of the SM. The exceptional group E_6 is one of the famous examples of this type. Phenomenologically, the most interesting option is the breaking of these U(1)'s at around TeV scales, giving rise to an extra neutral gauge boson observable at the Tevatron and the LHC. In a previous work [52], we considered a scenario of $\text{U}(1)'$ symmetry breaking at around TeV scale by the VEV of a Higgs singlet superfield in the context of weak-scale supersymmetry. The Z' boson obtains a mass from the breaking of this $\text{U}(1)'$ symmetry and proportional to the VEVs. Such a Z' can decay into the SUSY particles such as neutralinos, charginos, and sleptons, in addition to the SM particles. Thus, the current mass limits are reduced by a substantial amount and so is the sensitivity reach at the LHC [52, 53].

In this work, we turn our focus to the Higgs sector in UMSSM, which consists of 3 CP-even Higgs bosons, 1 CP-odd Higgs boson, and one pair of charged Higgs bosons. Because of the extra singlet Higgs superfield the mass of the lightest Higgs boson is raised by a substantial amount, easily to be above 130 GeV. However, for such a heavy Higgs boson, we have to hide it under the current data because the SM Higgs boson is ruled

JHEP06(2012)128

out for above 141 GeV [6, 7]. In UMSSM, there is an invisible decay mode of the SM-like Higgs boson into a pair of lightest neutralinos. We shall show that there are substantial parameter space that it is possible to hide the SM-like Higgs boson in this manner. On the other hand, if the SM-like Higgs boson lies in the lower mass range 120–131 GeV, we can find the parameter space that this SM-like Higgs boson decays in a manner similar to the SM Higgs boson, i.e., the decay branching ratios into $\gamma\gamma$, WW, ZZ, and $b\bar{b}$ are all similar to the SM values.

So what are the differences between the UMSSM and the other ones such as the next-to-minimal supersymmetric standard model (NMSSM)? There are a number of extensions to the MSSM by adding a Higgs singlet superfield depending on the different extra terms of the singlet in the superpotential (such as κS^3 of the NMSSM). However, these extensions often predict a light CP-odd Higgs boson, a light CP-even Higgs boson, and/or a light neutralino, in addition to those in the usual MSSM spectrum, such that the SM-like Higgs boson can decay into a pair of light pseudoscalar bosons, light Higgs bosons, or light neutralinos in some limits. If this is the case, the branching ratios into $\gamma\gamma$, WW, ZZ, and $b\bar{b}$ would diminish to small values, and so cannot explain the excess seen at the LHC. The point here is that not all Higgs-singlet extensions to the MSSM can account for the excess at the LHC, although most of them can raise the Higgs boson to the desirable value. The UMSSM, on the other hand, only has one CP-odd Higgs boson, which is MSSM-like. We will give more details, especially for NMSSM, in section 5.

We organize the paper as follows. In the next section, we describe the model briefly and work out the mass matrix of the CP-even Higgs bosons. In section 3, we list the formulas for the couplings of the CP-even Higgs bosons that are most relevant to our study. In section 4, we search for the parameter space in the model that can have a SM-like Higgs boson in the two mass ranges of (i) 130–141 GeV and (ii) 120–130 GeV, and show the branching ratios into WW, $b\bar{b}$, and $\tilde{\chi}_1^0\tilde{\chi}_1^0$. We discuss and conclude in section 5.

2 UMSSM

For illustration we use the popular grand unified models of E_6, which are anomaly-free. Two most studied U(1) subgroups in the symmetry breaking chain of E_6 are

$$E_6 \to \mathrm{SO}(10) \times \mathrm{U}(1)_\psi\,, \qquad \mathrm{SO}(10) \to \mathrm{SU}(5) \times \mathrm{U}(1)_\chi\,.$$

In E_6 each family of the left-handed fermions is promoted to a fundamental **27**-plet, which decomposes under $E_6 \to \mathrm{SO}(10) \to \mathrm{SU}(5)$ as

$$\mathbf{27} \to \mathbf{16} + \mathbf{10} + \mathbf{1} \to (\mathbf{10} + \mathbf{5}^* + \mathbf{1}) + (\mathbf{5} + \mathbf{5}^*) + \mathbf{1}\,.$$

We require one of the U(1)'s remains unbroken until around TeV scale, and then broken to give masses to the Z' boson and its superpartner Z'-ino. Each **27** contains the SM fermions, two additional singlets ν^c (conjugate of the right-handed neutrino) and S, a D and D^c pair (D is the exotic color-triplet quark with charge $-1/3$ and D^c is the conjugate), and a pair of color-singlet SU(2)-doublets H_u and H_d with hypercharge $Y_{H_u,H_d} = \pm 1/2$.

JHEP06(2012)128

SO(16)	SU(5)	$2\sqrt{10}Q'_\chi$	$2\sqrt{6}Q'_\psi$	$2\sqrt{15}Q'_\eta$	$2Q'_I$	$2\sqrt{10}Q'_N$	$2\sqrt{15}Q'_{\rm sec}$
16	$\mathbf{10}(u, d, u^c, e^c)$	-1	1	-2	0	1	$-1/2$
	$\mathbf{5}^*(d^c, \nu, e^-)$	3	1	1	-1	2	4
	ν^c	-5	1	-5	1	0	-5
10	$\mathbf{5}(D, H_u)$	2	-2	4	0	-2	1
	$\mathbf{5}^*(D^c, H_d)$	-2	-2	1	1	-3	$-7/2$
1	$\mathbf{1}S$	0	4	-5	-1	5	5/2

Table 1. The chiral charges of the left-handed fermions for various Z' models arised in E_6 [51]. Note that $Q'_{f_R} = -Q'(f^c)$ since all the right-handed SM fermions are necessarily charge-conjugated to convert into left-handed fields in order to put them into the irreducible representation of **27** of E_6.

In the supersymmetric version of E_6, the scalar components of one $H_{u,d}$ pair (out of 3 if there are 3 families) can be used as the two Higgs doublets $H_{u,d}$ of the MSSM. The chiral charges $\mathrm{U}(1)_\chi$ and $\mathrm{U}(1)_\psi$ for each member of the **27** are listed, respectively, in the third and fourth columns in table 1. In general, the two $\mathrm{U}(1)_\psi$ and $\mathrm{U}(1)_\chi$ can mix to form

$$Q'(\theta_{E_6}) = \cos\theta_{E_6} Q'_\chi + \sin\theta_{E_6} Q'_\psi \ , \tag{2.1}$$

where $0 \le \theta_{E_6} < \pi$ is the mixing angle. A commonly studied model is the Z'_η model with

$$Q'_\eta = \sqrt{\frac{3}{8}} Q'_\chi - \sqrt{\frac{5}{8}} Q'_\psi \ , \tag{2.2}$$

which has $\theta_{E_6} = \pi - \tan^{-1}\sqrt{5/3} \sim 0.71\pi$. There are also the inert model with $Q'_I = -Q'(\theta_{E_6} = \tan^{-1}\sqrt{3/5} \sim 0.21\pi)$, the neutral N model with $\theta_{E_6} = \tan^{-1}\sqrt{15} \sim 0.42\pi$, and the secluded sector model with $\theta_{E_6} = \tan^{-1}\sqrt{15}/9 \sim 0.13\pi$. The chiral charges for each member of the **27** are also listed in the last four columns in table 1 for these four variations of Z' models within E_6. Here we take the assumption that all the exotic particles, other than the particle contents of the MSSM, are very heavy and well beyond the reaches of all current and planned colliders. For an excellent review of Z' models, see ref. [51].

The effective superpotential $W_{\rm eff}$ involving the matter and Higgs superfields in UMSSM can be written as

$$W_{\rm eff} = \epsilon_{ab}\left[y^u_{ij} Q^a_j H^b_u U^c_i - y^d_{ij} Q^a_j H^b_d D^c_i - y^l_{ij} L^a_j H^b_d E^c_i + h_s S H^a_u H^b_d\right] \ , \tag{2.3}$$

where $\epsilon_{12} = -\epsilon_{21} = 1$, i, j are family indices, and y^u and y^d represent the Yukawa matrices for the up-type and down-type quarks respectively. Here Q, L, U^c, D^c, E^c, H_u, and H_d denote the MSSM superfields for the quark doublet, lepton doublet, up-type quark singlet, down-type quark singlet, lepton singlet, up-type Higgs doublet, and down-type Higgs doublet respectively, and the S is the singlet superfield. Note that we have assumed other exotic fermions are so heavy that they have been integrated out and do not enter into the above effective superpotential. The $\mathrm{U}(1)'$ charges of the fields H_u, H_d, and S are related

JHEP06(2012)128

by $Q'_{H_u} + Q'_{H_d} + Q'_S = 0$ such that SH_uH_d is the only term allowed by the U(1)′ symmetry beyond the MSSM. Once the singlet scalar field S develops a VEV, it generates an effective μ parameter: $\mu_{\rm eff} = h_s\langle S\rangle$. The case is very similar to NMSSM, except we do not have the cubic term S^3 since it is forbidden by the U(1)′ symmetry.

The singlet superfield will give rise to a singlet scalar boson and a singlino. The real part of the scalar boson will mix with the real part of H_u^0 and H_d^0 to form 3 CP-even Higgs boson. The imaginary part of the singlet scalar will be eaten in the process of U(1)′ symmetry breaking and becomes the longitudinal part of the Z' boson. The singlino, together with the Z'-ino, will mix with the neutral gauginos and neutral Higgsinos to form 6 neutralinos. Studies of various singlet-extensions of the MSSM can be found in refs. [59–63]. At or below TeV scale the particle content is almost the same as the MSSM, except that it has 3 CP-even Higgs boson, 1 CP-odd Higgs boson, and a pair of charged Higgs boson in the Higgs sector, and also a Z' boson and 2 extra neutralinos (coming from the Z'-ino and the singlino.)

The gauge interactions involving the fermionic and scalar components, denoted generically by ψ and ϕ respectively, of each superfield are

$$\mathcal{L} = \frac{1}{2}\bar{\psi}_i\, i\gamma^\mu D_\mu\, \psi_i + (D^\mu\phi_i)^\dagger\, (D_\mu\phi_i)\ , \tag{2.4}$$

where ψ_i and ϕ_i denote the Majorana fermionic and bosonic components of the superfield, respectively. The covariant derivative of ϕ_i is given by

$$D_\mu\phi_i = \left[\partial_\mu + ieQA_\mu + i\frac{g}{\sqrt{2}}(\tau^+W_\mu^+ + \tau^-W_\mu^-) + ig_1(T_{3L} - Qx_{\rm w})Z_\mu + ig_2Z'_\mu Q'\right]\ \phi_i\ . \tag{2.5}$$

Here e is the electromagnetic coupling constant, Q is the electric charge, g is the $\mathrm{SU}(2)_L$ coupling, $\tau^\pm$ are the rising and lowering operators on weak doublets, T_{3L} is the third component of the weak isospin, and Q' is the chiral charges of the U(1)′ associated with the Z' boson. The interactions of Z' with all MSSM fields go through eqs. (2.4) and (2.5). The chiral charges of various Z' models are listed in tables 1. The coupling constant g_1 in eq. (2.5) is the SM coupling $g/\cos\theta_{\rm w}$, while in grand unified theories (GUT) g_2 is related to g_1 by

$$\frac{g_2}{g_1} = \left(\frac{5}{3}\,x_{\rm w}\lambda\right)^{1/2} \simeq 0.62\lambda^{1/2}\,, \tag{2.6}$$

where $x_{\rm w} = \sin^2\theta_{\rm w}$ and $\theta_{\rm w}$ is the weak mixing angle. The factor λ depends on the symmetry breaking pattern and the fermion sector of the theory, which is usually of order unity.

The Higgs doublet and singlet fields are

$$H_d = \begin{pmatrix} H_d^0 \\ H_d^- \end{pmatrix}\ , \qquad H_u = \begin{pmatrix} H_u^+ \\ H_u^0 \end{pmatrix} \qquad \text{and} \qquad S\ . \tag{2.7}$$

The scalar interactions are obtained by calculating the F- and D-terms of the superpotential, and by including the soft-SUSY-breaking terms. The terms involving the neutral components of the Higgs fields are

$$V_H = V_F + V_D + V_{\rm soft}\ , \tag{2.8}$$

JHEP06(2012)128

with

$$V_F = |-h_s H_u^0 H_d^0|^2 + |h_s S|^2(|H_u^0|^2 + |H_d^0|^2)\,, \tag{2.9}$$

$$V_D = \frac{g_1^2}{8}\left(|H_u^0|^2 - |H_d^0|^2\right)^2 + \frac{g_2^2}{2}\left(Q'_{H_u}|H_u^0|^2 + Q'_{H_d}|H_d^0|^2 + Q'_S|S|^2\right)^2\,, \tag{2.10}$$

$$V_{\rm soft} = M_{H_u}^2|H_u^0|^2 + M_{H_d}^2|H_d^0|^2 + M_S^2|S|^2 + (-h_s A_s S H_u^0 H_d^0 + \text{h.c.})\,. \tag{2.11}$$

The minimization conditions of $\partial V_H/\partial H_u^0 = 0$, $\partial V_H/\partial H_d^0 = 0$, and $\partial V_H/\partial S = 0$ at the vacuum give the following tadpole conditions:

$$\begin{aligned} M_{H_u}^2 = &-\frac{v_d^2}{2}\left(h_s^2 - \frac{g_1^2}{4} + g_2^2 Q'_{H_d}Q'_{H_u}\right) - \frac{v_u^2}{2}\left(\frac{g_1^2}{4} + g_2^2 Q'^2_{H_u}\right) - \frac{v_s^2}{2}\left(h_s^2 + g_2^2 Q'_S Q'_{H_u}\right) \\ &+ \frac{h_s A_s}{\sqrt{2}}\frac{v_s v_d}{v_u}\,, \end{aligned} \tag{2.12}$$

$$\begin{aligned} M_{H_d}^2 = &-\frac{v_d^2}{2}\left(\frac{g_1^2}{4} + g_2^2 Q'^2_{H_d}\right) - \frac{v_u^2}{2}\left(h_s^2 - \frac{g_1^2}{4} + g_2^2 Q'_{H_u}Q'_{H_d}\right) - \frac{v_s^2}{2}\left(h_s^2 + g_2^2 Q'_S Q'_{H_d}\right) \\ &+ \frac{h_s A_s}{\sqrt{2}}\frac{v_s v_u}{v_d}\,, \end{aligned} \tag{2.13}$$

$$M_S^2 = -\frac{v_d^2}{2}\left(h_s^2 + g_2^2 Q'_{H_d}Q'_S\right) - \frac{v_u^2}{2}\left(h_s^2 + g_2^2 Q'_{H_u}Q'_S\right) - \frac{v_s^2}{2}g_2^2 Q'^2_S + \frac{h_s A_s}{\sqrt{2}}\frac{v_u v_d}{v_s}\,. \tag{2.14}$$

where $\langle H_u^0\rangle = v_u/\sqrt{2}$, $\langle H_d^0\rangle = v_d/\sqrt{2}$, and $\langle S\rangle = v_s/\sqrt{2}$ are the VEVs. The two VEVs v_u and v_d satisfy $v^2 \equiv v_u^2 + v_d^2 = (246\text{ GeV})^2$ and the ratio $\tan\beta \equiv v_u/v_d$ is commonly defined in the literature. Now we can expand the Higgs fields as

$$\begin{aligned} H_d^0 &= \frac{1}{\sqrt{2}}\left(v_d + \phi_d + i\chi_d\right)\,, \\ H_u^0 &= \frac{1}{\sqrt{2}}\left(v_u + \phi_u + i\chi_u\right)\,, \\ S &= \frac{1}{\sqrt{2}}\left(v_s + \phi_s + i\chi_s\right)\,, \end{aligned}$$

and substitute into V_F, V_D, and $V_{\rm soft}$. The tree level mass matrix $\mathcal{M}^{\rm tree}$ can be read off from the bilinear terms in the expansion, namely

$$V_{\rm mass} = \frac{1}{2}\left(\phi_d\,,\ \phi_u\,,\ \phi_s\right)\mathcal{M}^{\rm tree}\begin{pmatrix}\phi_d\\ \phi_u\\ \phi_s\end{pmatrix}\,, \tag{2.15}$$

with

$$\begin{aligned} \mathcal{M}_{11}^{\rm tree} &= \left(\frac{g_1^2}{4} + g_2^2 Q'^2_{H_d}\right)v_d^2 + \frac{h_s A_s}{\sqrt{2}}\frac{v_s v_u}{v_d}\,, \\ \mathcal{M}_{22}^{\rm tree} &= \left(\frac{g_1^2}{4} + g_2^2 Q'^2_{H_u}\right)v_u^2 + \frac{h_s A_s}{\sqrt{2}}\frac{v_s v_d}{v_u}\,, \\ \mathcal{M}_{33}^{\rm tree} &= g_2^2 Q'^2_S v_s^2 + \frac{h_s A_s}{\sqrt{2}}\frac{v_d v_u}{v_s}\,, \end{aligned}$$

JHEP06(2012)128

$$\mathcal{M}^{\rm tree}_{12} = \left(h_s^2 - \frac{g_1^2}{4} + g_2^2 Q'_{H_u} Q'_{H_d}\right) v_d v_u - \frac{h_s A_s}{\sqrt{2}} v_s = \mathcal{M}^{\rm tree}_{21} ,$$
$$\mathcal{M}^{\rm tree}_{13} = \left(h_s^2 + g_2^2 Q'_{H_d} Q'_S\right) v_d v_s - \frac{h_s A_s}{\sqrt{2}} v_u = \mathcal{M}^{\rm tree}_{31} ,$$
$$\mathcal{M}^{\rm tree}_{23} = \left(h_s^2 + g_2^2 Q'_{H_u} Q'_S\right) v_u v_s - \frac{h_s A_s}{\sqrt{2}} v_d = \mathcal{M}^{\rm tree}_{32} .$$

It is well-known that the lightest CP-even Higgs boson mass receives a substantial radiative mass correction in MSSM. The same is true here for the UMSSM. Radiative corrections to the mass matrix $\mathcal{M}^{\rm tree}$ have been given in ref. [61, 62]. We have included radiative corrections in our calculation. The real symmetric mass matrix $\mathcal{M} = \mathcal{M}^{\rm tree+radiative}$ can then be diagonalized by an orthogonal transformation

$$\begin{pmatrix} h_1 \\ h_2 \\ h_3 \end{pmatrix} = \mathcal{O} \begin{pmatrix} \phi_d \\ \phi_u \\ \phi_s \end{pmatrix} \qquad \text{or} \qquad \begin{pmatrix} \phi_d \\ \phi_u \\ \phi_s \end{pmatrix} = \mathcal{O}^T \begin{pmatrix} h_1 \\ h_2 \\ h_3 \end{pmatrix} , \tag{2.16}$$

such that $\mathcal{O}\mathcal{M}\mathcal{O}^T = \mathrm{diag}(m^2_{h_1},\ m^2_{h_2},\ m^2_{h_3})$ in ascending order. The mass spectra for the neutral CP-odd and the pair of charged Higgs bosons are the same as MSSM.

Note that the Higgs-boson masses receive extra contributions from the D-term of the U(1)′ symmetry (proportional to g_2) and from the F-term of the mixing with the singlet Higgs field (proportional to h_s). These two contributions have nontrivial enhancement or cancellation between them, especially when they are comparable. Since g_2 is more or less fixed by the GUT condition on the extra U(1)′, we can vary the size of the h_s to modify the relative contributions of the D-term and F-term. In section 4, we shall study the small case of $h_s = 0.1$ and the larger case of $h_s = 0.4$–0.6 in the scanning of parameter space.

3 Couplings relevant for Higgs decays

In this section, we present the neutral CP-even Higgs bosons couplings with the gauge bosons, quarks and neutralinos. Other couplings that are not relevant to this work will be omitted.

The interactions of physical Higgs bosons $h_{1,2,3}$ with SM particles and other SUSY particles can be obtained by writing down the Lagrangian in the weak eigenbasis and then rotating the Higgs weak eigenstates as

$$\begin{aligned} \phi_d &= \mathcal{O}_{11} h_1 + \mathcal{O}_{21} h_2 + \mathcal{O}_{31} h_3 \ , \\ \phi_u &= \mathcal{O}_{12} h_1 + \mathcal{O}_{22} h_2 + \mathcal{O}_{32} h_3 \ , \\ \phi_s &= \mathcal{O}_{13} h_1 + \mathcal{O}_{23} h_2 + \mathcal{O}_{33} h_3 \ . \end{aligned} \tag{3.1}$$

3.1 Higgs couplings to gauge bosons

The couplings of the Higgs bosons to a pair of gauge bosons come from $(D_\mu H_u)^\dagger (D^\mu H_u) + (D_\mu H_d)^\dagger (D^\mu H_d) + (D_\mu S)^\dagger (D^\mu S)$:

$$\mathcal{L}_{\rm gauge} = \mathcal{L}_{WW} + \mathcal{L}_{ZZ} + \mathcal{L}_{Z'Z'} + \mathcal{L}_{ZZ'} \ , \tag{3.2}$$

JHEP06(2012)128

where

$$\begin{aligned}
\mathcal{L}_{WW} &= \frac{g^2}{4} W_\mu^+ W^{-\mu} \left[v^2 + 2v_u\phi_u + 2v_d\phi_d + \cdots \right] \ , \\
&= m_W^2 W_\mu^+ W^{-\mu} + g m_W W_\mu^+ W^{-\mu} \left[(\sin\beta \mathcal{O}_{j2} + \cos\beta \mathcal{O}_{j1}) h_j + \cdots \right] \ , \qquad (3.3) \\
\mathcal{L}_{ZZ} &= \frac{g_1^2}{8} Z_\mu Z^\mu \left[v^2 + 2v_u\phi_u + 2v_d\phi_d + \cdots \right] \ , \\
&= \frac{m_Z^2}{2} Z_\mu Z^\mu + \frac{g_1}{2} m_Z Z_\mu Z^\mu \left[(\sin\beta \mathcal{O}_{j2} + \cos\beta \mathcal{O}_{j1}) h_j + \cdots \right] \ , \qquad (3.4) \\
\mathcal{L}_{Z'Z'} &= g_2^2 Z'_\mu Z'^\mu \left[Q'^2_{H_d} |H_d^0|^2 + Q'^2_{H_u} |H_u^0|^2 + Q'^2_S |S|^2 \right] \ , \\
&= \frac{1}{2} m_{Z'}^2 Z'_\mu Z'^\mu + g_2^2 Z'_\mu Z'^\mu h_j v \left[\sin\beta Q'^2_{H_u} \mathcal{O}_{j2} + \cos\beta Q'^2_{H_d} \mathcal{O}_{j1} + \frac{v_s}{v} Q'^2_S \mathcal{O}_{j3} \right] \ , \qquad (3.5) \\
\mathcal{L}_{ZZ'} &= 2 g_1 g_2 Z_\mu Z'^\mu \left[\frac{1}{2} Q'_{H_d} |H_d^0|^2 - \frac{1}{2} Q'_{H_u} |H_u^0|^2 \right] \ , \qquad (3.6) \\
&= \frac{g_1 g_2}{2} Z_\mu Z'^\mu \left[Q'_{H_d} v_d^2 - Q'_{H_u} v_u^2 \right] + g_1 g_2 Z_\mu Z'^\mu h_j v \left[\cos\beta Q'_{H_d} \mathcal{O}_{j1} - \sin\beta Q'_{H_u} \mathcal{O}_{j2} \right] \ ,
\end{aligned}$$

with $m_W = \frac{g}{2} v$, $m_Z = \frac{g_1}{2} v$ and $m_{Z'} \approx g_2 (Q'^2_{H_u} v_u^2 + Q'^2_{H_d} v_d^2 + Q'^2_s v_s^2)^{1/2}$ for small $Z - Z'$ mixing.

3.2 Yukawa couplings

Yukawa couplings are obtained by taking second order derivatives of the effective superpotential in eq. (2.3). The interactions only go through the Higgs doublets, given by

$$\begin{aligned}
\mathcal{L}_{\text{Yukawa}} &= -\frac{g m_u}{2 m_W \sin\beta} \bar{u} u \, \phi_u - \frac{g m_d}{2 m_W \cos\beta} \bar{d} d \, \phi_d \ , \\
&= -\frac{g m_u}{2 m_W \sin\beta} \mathcal{O}_{j2} \bar{u} u \, h_j - \frac{g m_d}{2 m_W \cos\beta} \mathcal{O}_{j1} \bar{d} d \, h_j \ , \qquad (3.7)
\end{aligned}$$

Similar formulas can be written down for the SM leptons.

3.3 Higgs couplings to the neutralinos

This is relevant when the lightest neutralino is very light such that the Higgs boson can decay into. The sources of neutralino masses come from soft masses of gauginos, from the superpotential term $h_s S H_u H_d$, and from those supersymmetric couplings $-\sqrt{2} g_a \phi^\dagger T^a \bar{\tilde{\lambda}} \psi$ ($\tilde{\lambda}$ is the Majorana gaugino field of a vector superfield, while ϕ and ψ are the scalar and fermionic components of a matter chiral superfield). The relevant terms for the masses are

$$\begin{aligned}
\mathcal{L}^{\text{mass}}_{\text{neutralinos}} = & -\frac{1}{2} M_1 \overline{\tilde{B}} \tilde{B} - \frac{1}{2} M_2 \overline{\tilde{W}^a} \tilde{W}^a - \frac{1}{2} M_{\tilde{Z}'} \overline{\tilde{Z}'} \tilde{Z}' \\
& - \frac{1}{2} \left[-\mu_{\text{eff}} \left(\overline{\tilde{h}_u^0} \tilde{h}_d^0 + \overline{\tilde{h}_d^0} \tilde{h}_u^0 \right) - \frac{h_s}{\sqrt{2}} v_u \left(\overline{\tilde{S}} \tilde{h}_d^0 + \overline{\tilde{h}_d^0} \tilde{S} \right) - \frac{h_s}{\sqrt{2}} v_d \left(\overline{\tilde{S}} \tilde{h}_u^0 + \overline{\tilde{h}_u^0} \tilde{S} \right) \right] \\
& - \frac{1}{2} \left[\frac{e}{2 c_w} v_u \left(\overline{\tilde{B}} \tilde{h}_u^0 + \overline{\tilde{h}_u^0} \tilde{B} \right) - \frac{e}{2 c_w} v_d \left(\overline{\tilde{B}} \tilde{h}_d^0 + \overline{\tilde{h}_d^0} \tilde{B} \right) - \frac{g}{2} v_u \left(\overline{\tilde{W}^3} \tilde{h}_u^0 + \overline{\tilde{h}_u^0} \tilde{W}^3 \right) \right. \\
& \quad + \frac{g}{2} v_d \left(\overline{\tilde{W}^3} \tilde{h}_d^0 + \overline{\tilde{h}_d^0} \tilde{W}^3 \right) + g_2 Q'_{H_u} v_u \left(\overline{\tilde{Z}'} \tilde{h}_u^0 + \overline{\tilde{h}_u^0} \tilde{Z}' \right) \qquad (3.8) \\
& \quad \left. + g_2 Q'_{H_d} v_d \left(\overline{\tilde{Z}'} \tilde{h}_d^0 + \overline{\tilde{h}_d^0} \tilde{Z}' \right) + g_2 Q'_S v_s \left(\overline{\tilde{Z}'} \tilde{S} + \overline{\tilde{S}} \tilde{Z}' \right) \right] \ .
\end{aligned}$$

JHEP06(2012)128

Thus the neutralino mass matrix $\mathcal{M}_N$ in the basis of $(\tilde{B},\, \tilde{W}^3,\, \tilde{h}_d^0,\, \tilde{h}_u^0,\, \tilde{S},\, \tilde{Z}')^T$ is given by [59, 60, 63]

$$\mathcal{M}_N = \left(\begin{array}{cccc|cc} M_1 & 0 & -\frac{e}{2c_w}v_d & \frac{e}{2c_w}v_u & 0 & 0 \\ 0 & M_2 & \frac{g}{2}v_d & -\frac{g}{2}v_u & 0 & 0 \\ -\frac{e}{2c_w}v_d & \frac{g}{2}v_d & 0 & -\mu_{\text{eff}} & -\frac{h_s}{\sqrt{2}}v_u & g_2 Q'_{H_d} v_d \\ \frac{e}{2c_w}v_u & -\frac{g}{2}v_u & -\mu_{\text{eff}} & 0 & -\frac{h_s}{\sqrt{2}}v_d & g_2 Q'_{H_u} v_u \\ \hline 0 & 0 & -\frac{h_s}{\sqrt{2}}v_u & -\frac{h_s}{\sqrt{2}}v_d & 0 & g_2 Q'_S v_s \\ 0 & 0 & g_2 Q'_{H_d} v_d & g_2 Q'_{H_u} v_u & g_2 Q'_S v_s & M_{\tilde{Z}'} \end{array}\right) . \tag{3.9}$$

The basis $(\tilde{B},\, \tilde{W}^3,\, \tilde{h}_d^0,\, \tilde{h}_u^0,\, \tilde{S},\, \tilde{Z}')^T$ is rotated into mass eigenstates $(\tilde{\chi}_1^0, \tilde{\chi}_2^0, \tilde{\chi}_3^0, \tilde{\chi}_4^0, \tilde{\chi}_5^0, \tilde{\chi}_6^0)^T$ by

$$(\tilde{B},\, \tilde{W}^3,\, \tilde{h}_d^0,\, \tilde{h}_u^0,\, \tilde{S},\, \tilde{Z}') = (\tilde{\chi}_1^0,\, \tilde{\chi}_2^0,\, \tilde{\chi}_3^0,\, \tilde{\chi}_4^0,\, \tilde{\chi}_5^0,\, \tilde{\chi}_6^0)\, N \tag{3.10}$$

and $N\mathcal{M}_N N^T = \text{diag}(M_{\tilde{\chi}_1^0}, M_{\tilde{\chi}_2^0}, M_{\tilde{\chi}_3^0}, M_{\tilde{\chi}_4^0}, M_{\tilde{\chi}_5^0}, M_{\tilde{\chi}_6^0})$ arranged in ascending order. N is a 6 by 6 orthogonal matrix since the neutralino mass matrix $\mathcal{M}_N$ is real and symmetric. The interactions between the CP-even Higgs boson and a pair of neutralinos are given by eq. (3.9) with the corresponding VEV replaced by ϕ (i.e. $v_{u,d,s} \longrightarrow \phi_{u,d,s}$). We can then rotate into mass eigenstates using (3.1) and the interaction terms are given by

$$\mathcal{L}^{\text{int}}_{\text{neutralinos}} = \frac{1}{2}\, h_k\, \overline{\tilde{\chi}_i^0}\, \left[\mathcal{H}^*_{ijk} P_L + \mathcal{H}_{ijk} P_R\right]\, \tilde{\chi}_j^0 \ , \tag{3.11}$$

with

$$\begin{aligned} \mathcal{H}_{ijk} = {} & \mathcal{O}_{k1}\left[\frac{h_s}{\sqrt{2}} N_{i5} N_{j4} + \frac{e}{2c_w} N_{i1} N_{j3} - \frac{g}{2} N_{i2} N_{j3} - g_2 Q'_{H_d} N_{i6} N_{j3}\right] \\ & + \mathcal{O}_{k2}\left[\frac{h_s}{\sqrt{2}} N_{i5} N_{j3} - \frac{e}{2c_w} N_{i1} N_{j4} + \frac{g}{2} N_{i2} N_{j4} - g_2 Q'_{H_u} N_{i6} N_{j4}\right] \\ & + \mathcal{O}_{k3}\left[\frac{h_s}{\sqrt{2}} N_{i4} N_{j3} - g_2 Q'_S N_{i6} N_{j5}\right] \\ & + \{i \leftrightarrow j\} \ . \end{aligned} \tag{3.12}$$

4 Scanning of parameter space

Besides the usual MSSM parameters of gaugino masses $M_{1,2,3}$, squark masses $M_{\tilde{q}}$, slepton masses $M_{\tilde{\ell}}$, A parameters $A_{t,b,\tau}$, and $\tan\beta$, the UMSSM has the following additional soft parameters: M_S, $M_{\tilde{Z}'}$, A_s, the VEV $\langle S\rangle = v_s/\sqrt{2}$, and the Yukawa coupling h_s. The effective μ parameter is given as $\mu_{\text{eff}} = h_s\langle S\rangle$. The other model parameters are fixed by the quantum numbers Q'_ϕ of various super-multiplets ϕ as given in table 1. The η model of E_6 defined by the generator in eq. (2.2) or by the fifth column for the **27** in table 1 will be used in the following for illustration.

Ignoring the $Z - Z'$ mixing, the mass of the Z' boson is determined by $m_{Z'} \approx g_2(Q'^2_{H_u} v_u^2 + Q'^2_{H_d} v_d^2 + Q'^2_s v_s^2)^{1/2}$. The most stringent limit on the Z' boson comes from the dilepton resonance search by ATLAS [64, 65]. The limits are 1.5–1.7 TeV for the various

JHEP06(2012)128

Z' bosons of the E_6 models. If the limits are translated into v_s using the above expression, the value of v_s has to be larger than a few TeV. Nevertheless, we can avoid these Z' mass limits by assuming the leptonic decay mode is suppressed. The mixing between the SM Z boson and the Z' can also be suppressed by carefully choosing the $\tan\beta \approx (Q'_{H_d}/Q'_{H_u})^{1/2}$. The goal of this work does not concern avoiding all these constraints, but we note that we can always carefully choose the set of quantum numbers Q' such that the Z' mass and mixing constraints can be evaded.

We first fix most of the MSSM parameters (unless stated otherwise):

$$\begin{aligned} &M_1 = 0.5 M_2 = 0.2 \text{ TeV}, \quad M_3 = 2 \text{ TeV} ; \\ &M_{\tilde{Q}} = M_{\tilde{U}} = A_t = 1 \text{ TeV}, \quad M_{\tilde{L}} = M_{\tilde{E}} = 0.2 \text{ TeV} . \end{aligned} \tag{4.1}$$

We also fix the following two UMSSM parameters

$$M_S = 0.5\,\text{TeV}, \quad A_s = 0.5\,\text{TeV} \ , \tag{4.2}$$

while we scan the rest of the parameters in the following ranges

$$0.2\,\text{TeV} < v_s < 2 \text{ TeV}, \quad 0.2 < h_s < 0.7, \quad 1.1 < \tan\beta < 40 \ , \ 0.2\,\text{TeV} < M_{\tilde{Z}'} < 2\,\text{TeV} \ . \tag{4.3}$$

Note that the U(1)$'$ gaugino mass, $M_{\tilde{Z}'}$, is a soft SUSY-breaking parameter, unlike the Z' boson mass which is fixed by the U(1)$'$ coupling constant and quantum numbers, and the VEVs.

4.1 Constraints

Charginos mass. The chargino sector of the UMSSM is the same as that of MSSM with the following chargino mass matrix

$$M_{\tilde{\chi}^\pm} = \begin{pmatrix} M_2 & \sqrt{2} m_W \sin\beta \\ \sqrt{2} m_W \cos\beta & \mu_{\text{eff}} \end{pmatrix} . \tag{4.4}$$

Thus, the two charginos masses depend on M_2, $\mu_{\text{eff}} = h_s v_s/\sqrt{2}$, and $\tan\beta$. The current bound is $M_{\tilde{\chi}^\pm} > 94\,\text{GeV}$ as long as the mass difference with the lightest supersymmetric particle (LSP) is larger than 3 GeV [66]. We impose this chargino mass bound in our scans in the parameter space defined by (4.3).

Invisible width of the Z boson. The lightest neutralino $\tilde{\chi}_1^0$ is the LSP of the model, and thus would be stable and invisible. When the Z boson decays into a pair of LSP, it would give rise to invisible width of the Z boson, which had been tightly constrained by experiments. The current bound of the Z invisible width is $\Gamma_{\text{inv}}(Z) < 3\,\text{MeV}$ at about 95% CL [66]. The coupling of the Z boson to the lightest neutralino is given by

$$\mathcal{L}_{Z\tilde{\chi}_1^0\tilde{\chi}_1^0} = \frac{g_1}{4} \left(|N_{13}|^2 - |N_{14}|^2 \right) Z_\mu \, \overline{\tilde{\chi}_1^0} \gamma^\mu \gamma_5 \, \tilde{\chi}_1^0 \, , \tag{4.5}$$

and the contribution to the Z boson invisible width is

$$\Gamma(Z \to \tilde{\chi}_1^0 \tilde{\chi}_1^0) = \frac{g_1^2}{96\pi} \left(|N_{13}|^2 - |N_{14}|^2 \right)^2 m_Z \left(1 - \frac{4 m_{\tilde{\chi}_1^0}^2}{m_Z^2} \right)^{3/2} . \tag{4.6}$$

JHEP06(2012)128

Here we impose the experimental constraint on the invisible Z width. The constraint of fulfilling the relic density by the LSP will be ignored in this work.

Current limits on the pseudoscalar Higgs bosons come from the LEP searches of $e^+e^- \to Z^* \to A_iH_j$, where i, j denote the mass eigenstates of the Higgs bosons; especially in those MSSM-extended models, such as NMSSM, with multiple pseudoscalar and scalar Higgs bosons the constraint could be severe. However, there is only one pseudoscalar Higgs boson in the UMSSM and in our choice of parameters it is often heavier than a few hundred GeV. Thus, it is not constrained by the current limits. Similarly, the charged Higgs boson is also heavy and not constrained by current searches.

4.2 The first scenario: $130 < M_{h_{\rm SM-like}} < 141\,\text{GeV}$

In Summer 2011, the LHC experiments reported a 2σ excess in the channel $h \to WW^* \to \ell^+\nu\ell^-\bar{\nu}$ ($\ell = e, \mu$) above the expected SM backgrounds, the implied Higgs boson mass is around 130–141 GeV and the branching ratio into WW^* is about 1/2 of the SM value [1–5]. Nevertheless, in December 2011 the most updated data [6, 7] indicated that SM Higgs boson above 131 GeV up to about 600 GeV is ruled out. It does not mean that a Higgs boson in the mass range above 131 GeV cannot exist, but just we have to find some ways to hide the Higgs boson. Therefore, when we scan for the SM-like Higgs boson in the mass range 130–141 GeV, we also search for the region that allows this Higgs boson to be invisible. We shall elaborate further about this below.

We first do the parameter space scan to search for the points that can give a SM-like Higgs boson of mass between 130 and 141 GeV. Here the SM-like Higgs boson is *not* always the lightest CP-even Higgs boson. Sometimes, the lightest Higgs boson is the singlet-like Higgs boson. We define the Higgs boson h_k to be SM-like by demanding the $O^2_{k3} < 0.1$ (where $h_k = O_{k1}\phi_d + O_{k2}\phi_u + O_{k3}\phi_s$). In our scan, we do not find more than one SM-like Higgs bosons. We show the points that pass the constraints of chargino mass, invisible Z width, and the mass of the SM-like Higgs boson between 130 and 141 GeV in figure 1 for a number of h_s values. It is obvious from the figure that a smaller h_s is more likely to give a Higgs boson in the mass range 130–141 GeV. The v_s is between 300 GeV and 1 TeV, and $\tan\beta$ is between 2 and 15. The variation of $M_{\tilde{Z}'}$ in our selected range is rather uniform and thus no preferred range of $M_{\tilde{Z}'}$. Note that for small $h_s = 0.1$ we do not find any parameter-space points for v_s up to 10 TeV in our scan that can give a SM-like Higgs boson in this mass range.

Once we have obtained the points with $M_{h_{\rm SM-like}}$ between 130 and 141 GeV, we can then calculate the branching ratios. In the mass range 130–141 GeV, the dominant decay modes of the SM-like Higgs boson include $b\bar{b}$, $\tau^+\tau^-$, WW^*, ZZ^*, and $\tilde{\chi}^0_1\tilde{\chi}^0_1$. Among these decay modes either $b\bar{b}$, WW^*, or $\tilde{\chi}^0_1\tilde{\chi}^0_1$ usually dominates. We found that if the SM-like Higgs boson is h_2, h_2 is always lighter than twice the lightest h_1 mass so that $h_2 \to h_1h_1$ is absent in our scan. We show in figure 2 the parameter space points obtained in figure 1 that have the branching ratio $B(h_{\rm SM-like} \to b\bar{b}) > 0.4$ in the first column, $B(h_{\rm SM-like} \to WW^*) > 0.4$ in the second column, and $B(h_{\rm SM-like} \to \tilde{\chi}^0_1\tilde{\chi}^0_1) > 0.4$ in the third column. The rows from top to bottom are for $h_s = 0.4$, 0.5, and 0.6, respectively. For smaller h_s the invisible mode is not as frequent as the other visible modes ($b\bar{b}$ and WW^*), while for larger h_s the invisible

JHEP06(2012)128

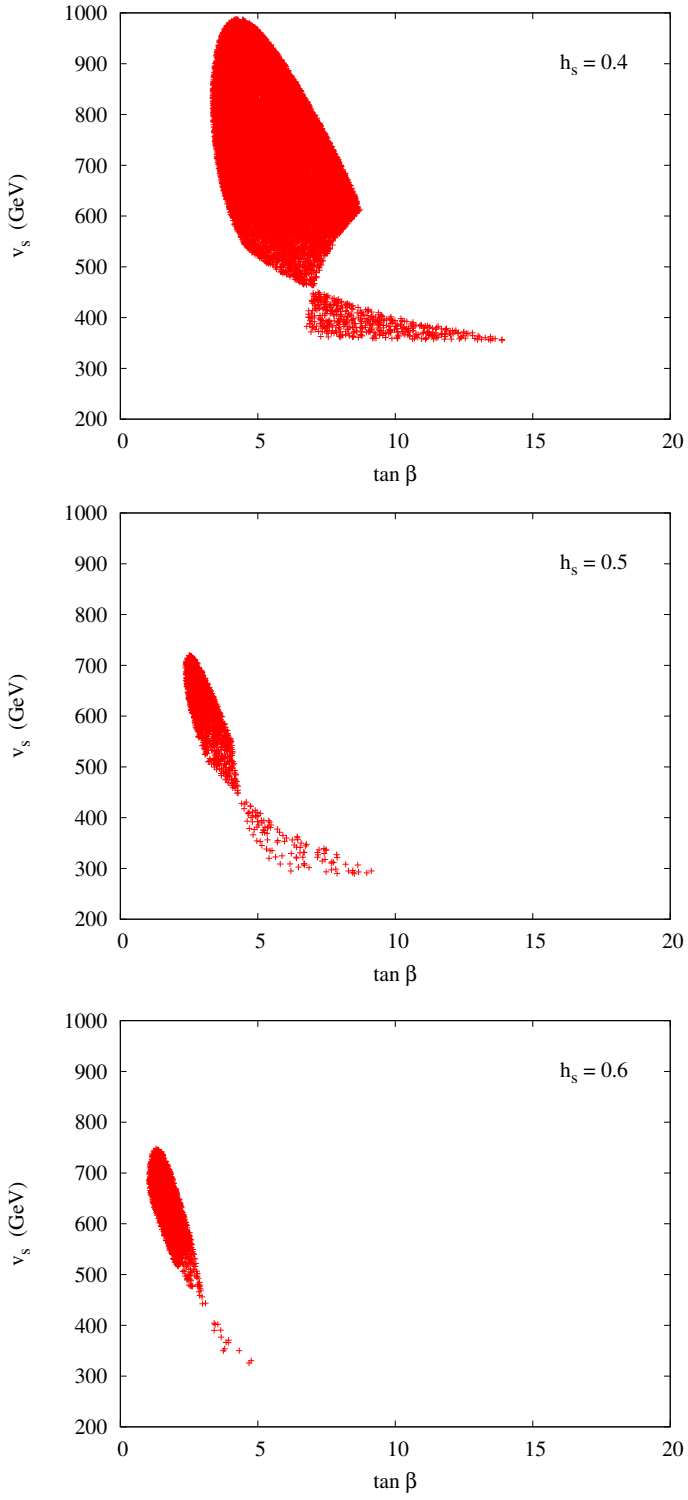

Figure 1. Two-dimensional scatter plots for the parameter-space points satisfying the chargino mass constraint $M_{\tilde{\chi}^{\pm}} > 94\,\text{GeV}$, invisible Z width less than 3 MeV, and $130 < M_{h_{\text{SM-like}}} < 141\,\text{GeV}$, where the SM-like Higgs boson $h_{\text{SM-like}}$ satisfies $O_{k3}^2 < 0.1$ (where $h_k = O_{k1}\phi_d + O_{k2}\phi_u + O_{k3}\phi_s$).

JHEP06(2012)128

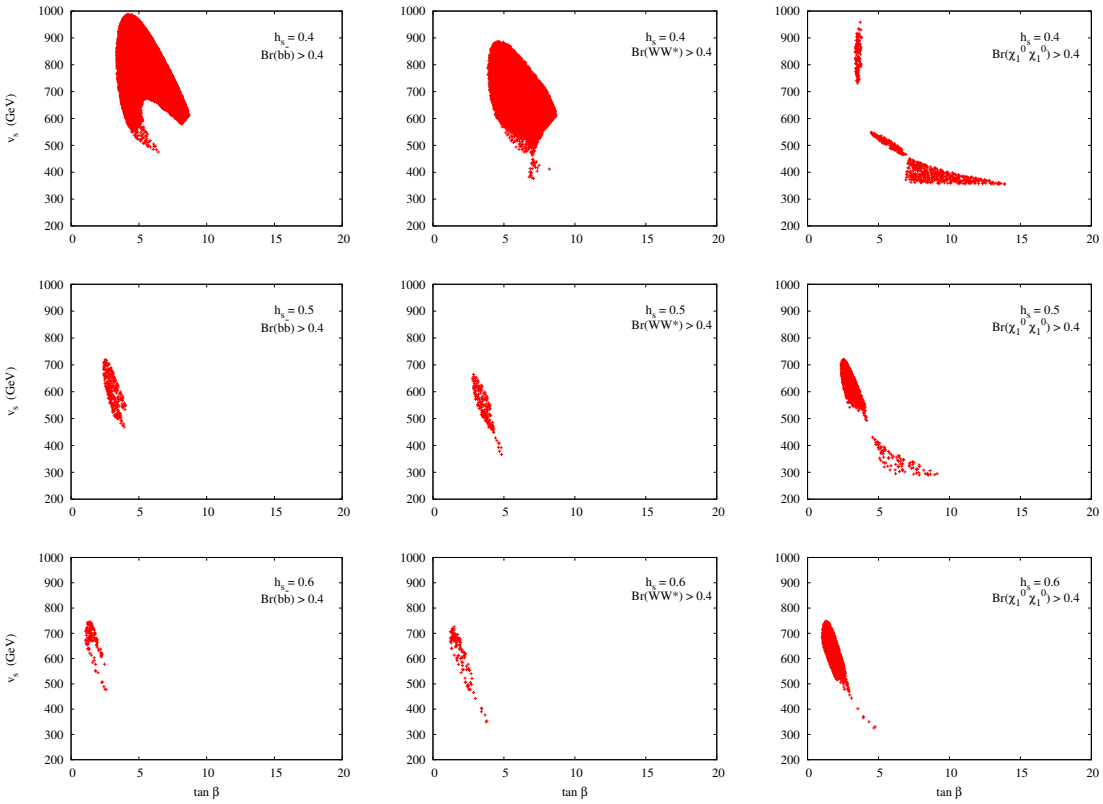

Figure 2. These scattered plots first pass the requirements of charginos masses $M_{\tilde{\chi}^\pm} > 94\,\text{GeV}$, the invisible Z width $\Gamma_{\text{inv}}(Z) < 3\,\text{MeV}$, and $130\,\text{GeV} < M_{h_{\text{SM-like}}} < 141$ GeV. The first row for $h_s = 0.4$, the second row for $h_s = 0.5$, and the third row for $h_s = 0.6$. The first column for $B(h_{\text{SM-like}} \to b\bar{b}) > 0.4$, the second column for $B(h_{\text{SM-like}} \to WW^*) > 0.4$, and the third column for $B(h_{\text{SM-like}} \to \tilde{\chi}_1^0\tilde{\chi}_1^0) > 0.4$.

mode is more frequent. In most recent results of ATLAS [6] and CMS [7], the SM Higgs boson above 130 GeV and up to about 600 GeV is ruled out. Possible ways out include adding invisible or dijet decay modes to the Higgs boson. Therefore, if a Higgs boson has an invisible decay mode with a branching ratio larger than about 0.4, it can survive the search limit from the LHC. The parameter space points with $B(h_{\text{SM-like}} \to \tilde{\chi}_1^0\tilde{\chi}_1^0) > 0.4$ presented here can then survive the LHC limits. So, the current LHC data prefers a larger h_s if the SM-like Higgs boson falls in the mass range of 130–141 GeV.

4.3 The second scenario: $120 < M_{h_{\text{SM-like}}} < 130\,\text{GeV}$

We repeat the whole exercise in the previous scenario with the new requirement of Higgs boson mass in the range $120 < M_{h_{\text{SM-like}}} < 130\,\text{GeV}$. We show the parameter space points that satisfy the chargino mass bound, Z invisible width, and $120 < M_{h_{\text{SM-like}}} < 130\,\text{GeV}$ in figure 3. It is also true for this mass range that a smaller h_s is easier to give a SM-like Higgs boson mass of 120–130 GeV. For $h_s = 0.4$ the v_s extends from 500 GeV to 2 TeV, and $\tan\beta$ from 2 to 18. For $h_s = 0.5, 0.6$ the ranges of v_s and $\tan\beta$ are substantially smaller. In figure 4, we show the parameter-space points that each branching ratio $B(b\bar{b}) > 0.3$,

JHEP06(2012)128

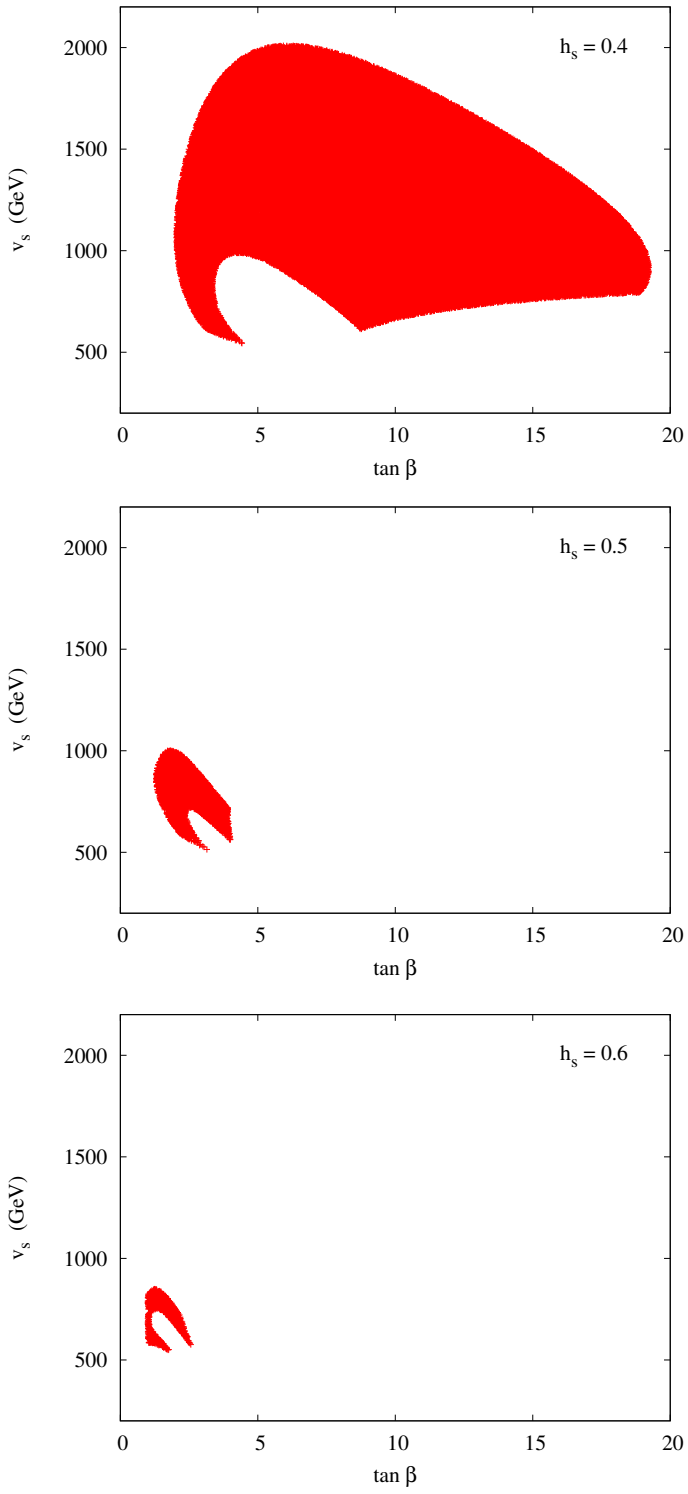

Figure 3. Two-dimensional scatter plots for the parameter-space points satisfying the chargino mass constraint $M_{\tilde{\chi}^{\pm}} > 94\,\text{GeV}$, invisible Z width less than 3 MeV, and $120 < M_{h_{\text{SM-like}}} < 130\,\text{GeV}$, where the SM-like Higgs boson $h_{\text{SM-like}}$ satisfies $O_{k3}^2 < 0.1$ (where $h_k = O_{k1}\phi_d + O_{k2}\phi_u + O_{k3}\phi_s$).

JHEP06(2012)128

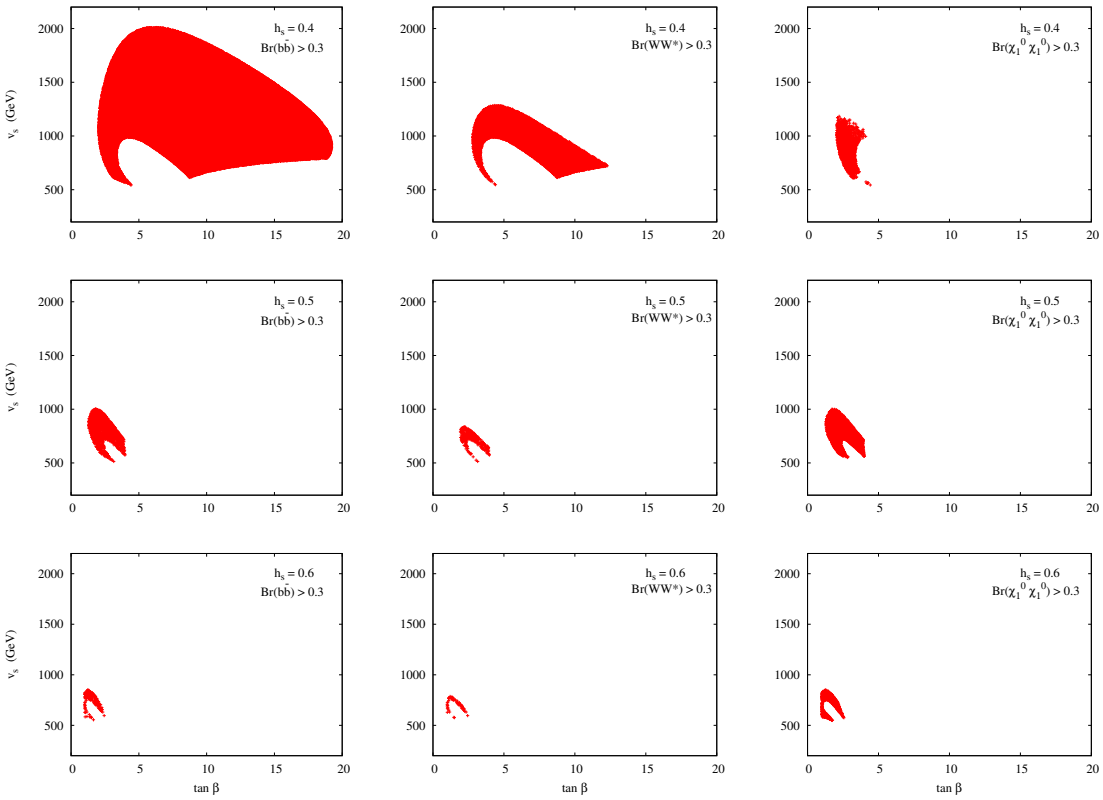

Figure 4. These scattered plots first pass the requirements of charginos masses $M_{\tilde{\chi}^\pm} > 94\,\text{GeV}$, the invisible Z width $\Gamma_{\text{inv}}(Z) < 3\,\text{MeV}$, and $120\,\text{GeV} < M_{h_{\text{SM-like}}} < 130$ GeV. The first row for $h_s = 0.4$, the second row for $h_s = 0.5$, and the third row for $h_s = 0.6$. The first column for $B(h_{\text{SM-like}} \to b\bar{b}) > 0.3$, the second column for $B(h_{\text{SM-like}} \to WW^*) > 0.3$, and the third column for $B(h_{\text{SM-like}} \to \tilde{\chi}_1^0\tilde{\chi}_1^0) > 0.3$.

$B(WW^*) > 0.3$, and $B(\tilde{\chi}_1^0\tilde{\chi}_1^0) > 0.3$. We used 0.3 in this figure because the points for WW and $\tilde{\chi}_1^0\tilde{\chi}_1^0$ would be very few if we chose 0.4. At such a low-mass range the $b\bar{b}$ often dominates over the WW^*, and the $b\bar{b}$ mode also dominates over $\tilde{\chi}_1^0\tilde{\chi}_1^0$ for $h_s = 0.4$; while for $h_s = 0.5$ and 0.6, the $\tilde{\chi}_1^0\tilde{\chi}_1^0$ mode is indeed dominant. This feature is similar to the other mass range 130–141 GeV: when h_s is large the invisible mode becomes more important. Therefore, the current LHC data prefers a smaller h_s if the SM-like Higgs boson falls in the mass range of 120–130 GeV. Note that the indent in the red area in each panel of figure 3 ($h_s = 0.4, 0.5, 0.6$) is very close to the corresponding red region of figure 1.

Another feature of the current LHC data showed that the production rate of the Higgs boson into diphotons is slightly larger than that of the SM Higgs boson [6, 7]. However, one has to be careful that the current data consists of large statistical uncertainties, and the data are consistent either with the presence of the SM Higgs boson or without any Higgs boson. It has been shown in a number of recent works that in MSSM [37–44] or NMSSM [55–57] the production rate of diphotons is similar to that of the SM Higgs boson, mostly slightly smaller than the SM one, though at some points in the parameter space it could be slightly larger. Nevertheless, under some less restrictive conditions the production

JHEP06(2012)128

rate of diphotons may be enhanced by up to a factor of 2 in the NMSSM [56, 57]. Here, we do not expect the UMSSM can give a dramatic change in diphoton production rate, as long as the SM-like Higgs boson does not decay into the lightest neutralinos. We show those points that have substantial branching ratios into $b\bar{b}$ and WW in figure 4 (first and second column). In this case, the production rate into diphotons would not be any different from the MSSM predictions, because the gluon-fusion is very similar and so is the decay into diphotons, except for a slight singlet component in the Higgs boson couplings. Therefore, in this subsection we have shown the parameter space of UMSSM that can give a SM-like Higgs boson of mass 120–130 GeV with branching ratios similar to those of the SM Higgs boson. On the other hand, we also show the parameter space points that the SM-like Higgs boson decays mostly into invisible neutralinos in the last column of figure 4.

4.4 Understanding the above results

In order to understand the indent regions in figure 3, we look at the variation of the Higgs boson masses M_{h_i} versus $\tan\beta$ at a fixed v_s and versus v_s at a fixed $\tan\beta$. The values of v_s and $\tan\beta$ fixed are suggested by figure 1 and the indents of figure 3. We choose $h_s = 0.4$ to illustrate the clearest feature of the variation. We first fix $v_s = 750\,\text{GeV}$ and vary $\tan\beta$, we plot M_{h_1} and M_{h_2} in figure 5a. Next, we fix $\tan\beta = 5$ and vary v_s and plot M_{h_1} and M_{h_2} in figure 5b. The M_{h_3} is basically outside the scale of the graphs. Also, we show the singlet fraction ($|O_{k3}|^2$) of each Higgs boson h_k in figure 5c. It is obvious that a crossing occurs slightly below $v_s = 500\,\text{GeV}$. The Higgs boson h_1 is mostly a singlet at small v_s and would not satisfy the requirement for a SM-like Higgs boson below 500 GeV at $\tan\beta = 5$. As v_s increases slightly above 500 GeV, the h_1 becomes mostly a nonsinglet ($|O_{13}|^2 < 0.1$).

Let us look more carefully at figure 5b, where a crossing between h_1 and h_2 occurs. At low v_s, the h_1 starts mostly a singlet while h_2 starts mostly a H_u. When v_s approaches 500 GeV, the role of singlet and H_u is reversed. After the crossing h_1 becomes mostly a H_u while h_2 becomes mostly a singlet. Because of the crossing, there exists a peak for M_{h_1}. We also indicate the horizontal lines of 120, 130, and 141 GeV. The peak of M_{h_1} in figure 5b clearly shows that the M_{h_1} can be above 130 GeV. That is the reason why when we traverse from small v_s to large v_s at $\tan\beta = 5$ in figure 3a, we come across an indent region from $v_s = 500\,\text{GeV}$ to about 1000 GeV, which corresponds to the SM-like Higgs mass heavier than 130 GeV. This is the red region in figure 1a. As v_s goes beyond 1000 GeV, the M_{h_1} falls in the range of 120 to 130 GeV. We now look at figure 5a. When we traverse from small $\tan\beta$ to large $\tan\beta$ at $v_s = 750\,\text{GeV}$, the region from $\tan\beta = 3.5$ to 7 corresponds to the SM-like Higgs boson heavier than 130 GeV, which then explains the indent region in figure 3a. Similar behavior is expected for the cases of $h_s = 0.5$ and 0.6.

Next, we try to understand the trend of the SM-like Higgs boson mass shown in figures 1 and 3. We pick a parameter-space point at $\tan\beta = 2.5$ and $v_s = 600\,\text{GeV}$ and show the variations of M_{h_i} versus h_s in figure 6a. Roughly, M_{h_1} rises linearly from $h_s = 0.2{-}0.5$, then levels off at around 0.5 and drops after $h_s = 0.55$, because there appears a broad mixing between h_1 and h_2 around 0.55. If we look at the point $\tan\beta = 2.5$ and $v_s = 600\,\text{GeV}$ in parts (a) to (c) of figure 1, this point is outside the red region in part (a) because it is too light while it is inside the red region in parts (b) and (c), as shown in figure 6a.

JHEP06(2012)128

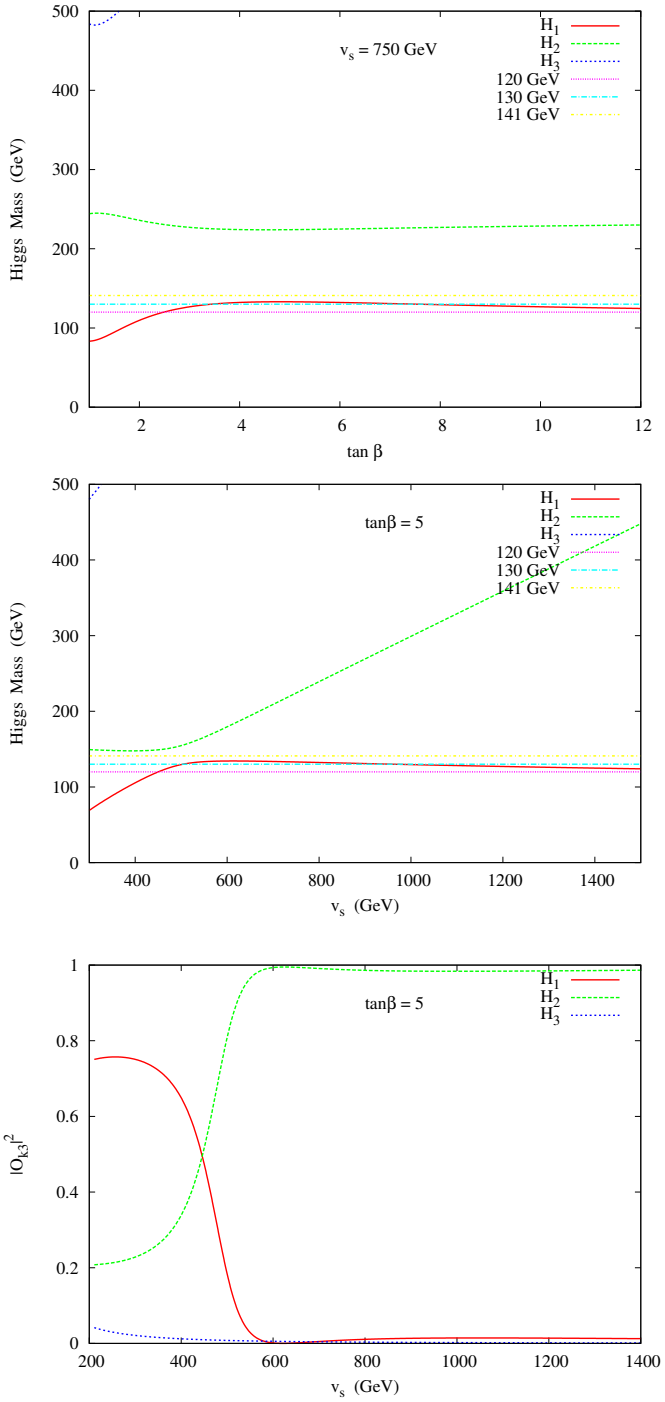

Figure 5. (a) The Higgs boson masses for h_1 and h_2 (h_3 is mostly outside the scale) versus $\tan\beta$ at $v_s = 750\,\text{GeV}$. The other parameters are fixed as in the text. Horizontal lines of 120, 130, and 141 GeV are also shown. (b) The Higgs boson masses for h_1 and h_2 versus v_s at $\tan\beta = 5$. (c) The singlet fraction ($|O_{k3}|^2$) of each Higgs boson versus v_s.

JHEP06(2012)128

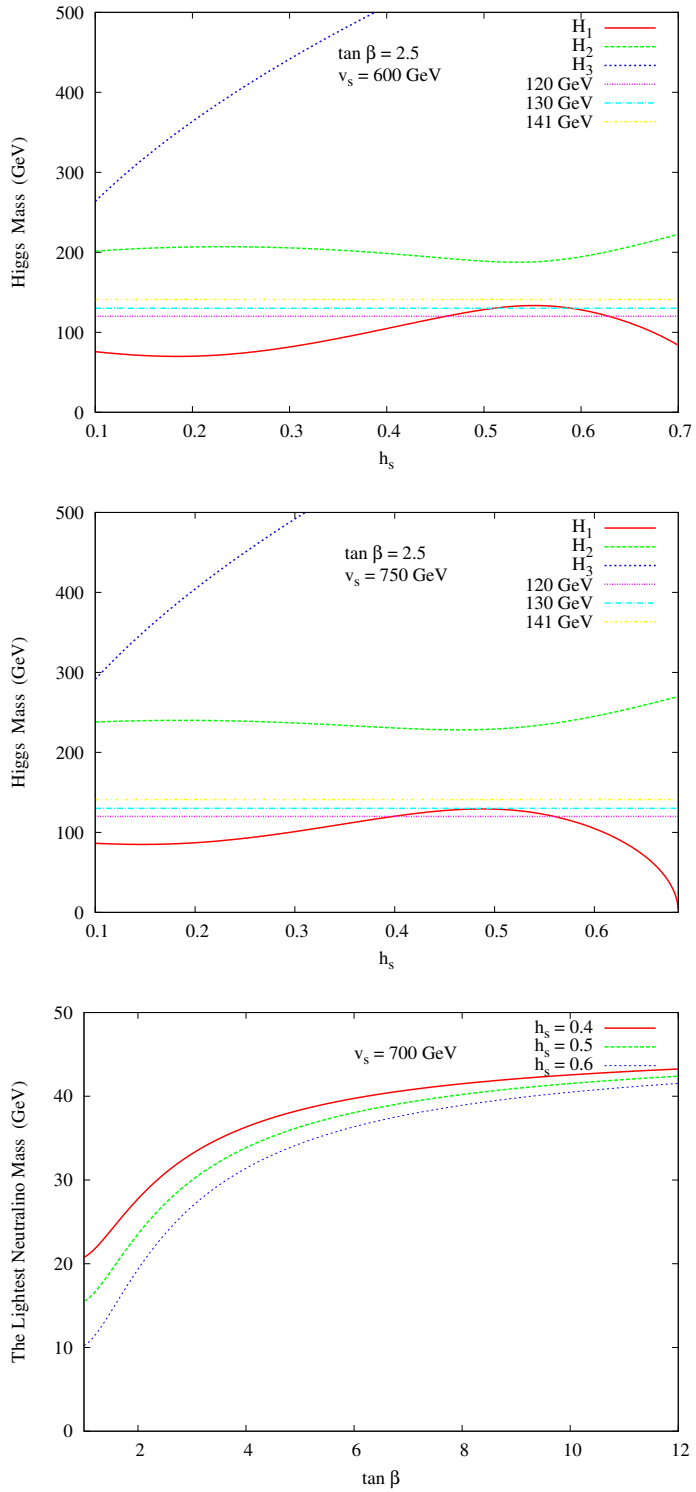

Figure 6. (a) The Higgs boson masses for h_1, h_2, and h_3 versus h_s at $\tan\beta = 2.5$ and $v_s = 600\,\text{GeV}$. (b) Same as part (a) but at $v_s = 750\,\text{GeV}$. (c) The lightest neutralino mass versus $\tan\beta$ at $v_s = 700\,\text{GeV}$. All other parameters are as in the text.

JHEP06(2012)128

Another parameter-space point $\tan\beta = 2.5$ and $v_s = 750\,\text{GeV}$ is shown in figure 6b. It also show similar behavior to figure 6a. A broad crossing occurs at $h_s \approx 0.5$, such that the M_{h_1} roughtly increases linearly from $h_s = 0.2 - 0.5$, then drops afterwards. If we look at the point $\tan\beta = 2.5$ and $v_s = 750\,\text{GeV}$ in parts (a) to (c) of figure 3, this point is inside the red region of parts (a) and (b) but outside part(c), as shown in figure 6b.

Further information can be obtained from figure 5a and 5b that the M_{h_1} in general increases with v_s and $\tan\beta$ before reaching the peak, then drops versus $\tan\beta$ and v_s after the peak. At $\tan\beta = 2.5$, $v_s = 600\,\text{GeV}$, and $h_s = 0.4$ (figure 6a) the M_{h_1} is still below 120 GeV, therefore it has plenty of parameter space to extend. Immediately, from figure 6b we can see that at $\tan\beta = 2.5$, $v_s = 750\,\text{GeV}$, and $h_s = 0.4$, M_{h_1} climbs to about 120 GeV. It still has a large parameter space to extend such that M_{h_1} is still above 120 GeV. On the other hand, at $\tan\beta = 2.5$, $v_s = 600\,\text{GeV}$, and $h_s = 0.5$ the M_{h_1} is close to 130 GeV (see figure 6a); and at $\tan\beta = 2.5$, $v_s = 750\,\text{GeV}$, and $h_s = 0.5$ the M_{h_1} already starts to drop (see figure 6b). Therefore, it has less parameter space to extend such that the M_{h_1} is above 120 GeV. Furthermore, it is clear that at $\tan\beta = 2.5$, $v_s = 600\,\text{GeV}$, and $h_s = 0.6$ the M_{h_1} already drops (see figure 6a) and falls below 120 GeV at $\tan\beta = 2.5$, $v_s = 750\,\text{GeV}$, and $h_s = 0.6$ (see figure 6b). Therefore, it has much less parameter space to extend such that the M_{h_1} is above 120 GeV. Hence, we can understand why the red regions in figures 1 and 3 shrink when h_s goes from 0.4 to 0.6.

The next part we want to understand is the trend of branching ratios shown in figures 2 and 4. As we shall discuss in the next section some nonstandard decay modes of the SM-like Higgs boson, once the Higgs boson can decay into a pair of neutralinos, it will dominate over the other standard decay modes of the Higgs boson. This is mainly because the decays into fermions are suppressed by Yukawa couplings and the decays into WW^* and ZZ^* are still suppressed by phase space for a 120–141 GeV Higgs boson; while the coupling of the Higgs boson to neutralinos is of order of weak interaction. Therefore, once the decay into a pair of neutralinos is kinematically allowed it will dominate over the other decay modes. In other words, we are trying to understand the trend of the mass of the lightest neutralino versus h_s. We show the mass of the lightest neutralino versus $\tan\beta$ for $h_s = 0.4 - 0.6$ in figure 6c. It is clear that the lightest neutralino mass increases with $\tan\beta$, and so the decay into a pair of neutralinos is not possible for a large enough $\tan\beta$. Furthermore, from figure 6c we can see that $h_s = 0.4$ will give a larger neutralino mass than $h_s = 0.5$ and $h_s = 0.6$. Therefore, we can see in figures 2 and 4 that the SM-like Higgs boson decays into a pair of neutralinos more frequently for $h_s = 0.6$ than for $h_s = 0.5$ and 0.4.

This can also be understood from the following approximate formula for the lightest neutralino in UMSSM, in the case that the singlet mass is smaller than the other components and the mixing between the upper 4×4 and the lower 2×2 blocks of the neutralino-mass matrix is small: [63]

$$M_{\tilde{\chi}_1^0} = \left| -\frac{Q_S'^2 g_2^2 v_s^2}{M_{\tilde{Z}'}} + \frac{h_s v^2}{v_s\sqrt{2}} \sin 2\beta \right| . \tag{4.7}$$

The first term is negative and numerically larger than the second term for our choice of parameters. Therefore, when h_s increases from 0.4 to 0.5 or 0.6, the second term becomes

JHEP06(2012)128

larger and the sum is numerically smaller. This explains the curves in figure 6c. For a fixed $\tan\beta$ the lightest neutralino mass decreases as h_s increases from 0.4 to 0.6, thus the SM-like Higgs boson has a larger chance to decay into a pair of neutralinos. This explains the trend seen in figures 2 and 4.

4.5 The case for $h_s = 0.1$

In the last subsection, we have seen nontrivial enhancement or cancellation between the D-term and F-term contributions. When h_s decreases from 0.6 to 0.4, more parameter-space points satisfy the mass range of $120 < M_{h_{\rm SM-like}} < 130\,{\rm GeV}$, as shown in figure 3. However, the trend is not trivial. We show the case of $h_s = 0.1$ in figure 7. In the panel (a), the red dots are the points that satisfy the mass range of $120 < M_{h_{\rm SM-like}} < 130\,{\rm GeV}$ with the constraints of invisible Z decay and chargino mass. It shows that a relatively larger value of v_s is required. In the panels (b) and (c), we show the points with $B(h_{\rm SM-like} \to b\bar{b}) > 0.3$ and $B(h_{\rm SM-like} \to W^+W^-) > 0.3$, respectively; while we do not find any points with $B(h_{\rm SM-like} \to \tilde{\chi}_1^0\tilde{\chi}_1^0) > 0.3$. Therefore, this SM-like Higgs boson behaves like a SM Higgs boson. This is to be contrasted with the case of $h_s = 0.4 - 0.6$, in which we have to avoid the decay $h_{\rm SM-like} \to \tilde{\chi}_1^0\tilde{\chi}_1^0$, otherwise the Higgs would be invisible.

5 Discussion

In principle, in both scenarios studied in the previous section, there may be some parameter space that the second lightest Higgs boson is SM-like and can also decay into the lightest Higgs boson, which is mostly singlet-like. However, in our scan we do not find such parameter-space points.

Comparison with the SM Higgs boson. If the SM Higgs boson falls in the mass range of larger than 130 GeV, it would be inconsistent with the current data [6, 7]. The UMSSM, on the other hand, can allow the SM-like Higgs boson in this mass range to decay invisibly into the lightest neutralinos, such that it can hide from the current data. The SM-like Higgs boson in the UMSSM can also accommodate in the lighter mass range of 120–130 GeV with the decay branching ratios very similar to those in the SM.

Comparison with the MSSM. The low energy spectrum of UMSSM has an extra CP-even Higgs boson and two more neutralinos. We have shown that the SM-like Higgs boson is most of the time the second lightest Higgs boson while the lightest one is more singlet-like. The singlet-like neutralino can be substantially lighter than the MSSM lightest neutralino, such that the SM-like Higgs boson can decay invisibly more frequently once this mode is open, but not quite so in the MSSM.

Comparison with the NMSSM. In terms of particle content, the major differences between UMSSM and NMSSM include

- NMSSM has two pseudoscalar Higgs bosons while UMSSM only has one, because the would-be-Goldstone boson becomes the longitudinal component of the Z' boson.
- NMSSM has five neutralinos with the extra one coming from the singlino while UMSSM has six neutralinos with additional ones from the singlino and Z'-ino.

JHEP06(2012)128

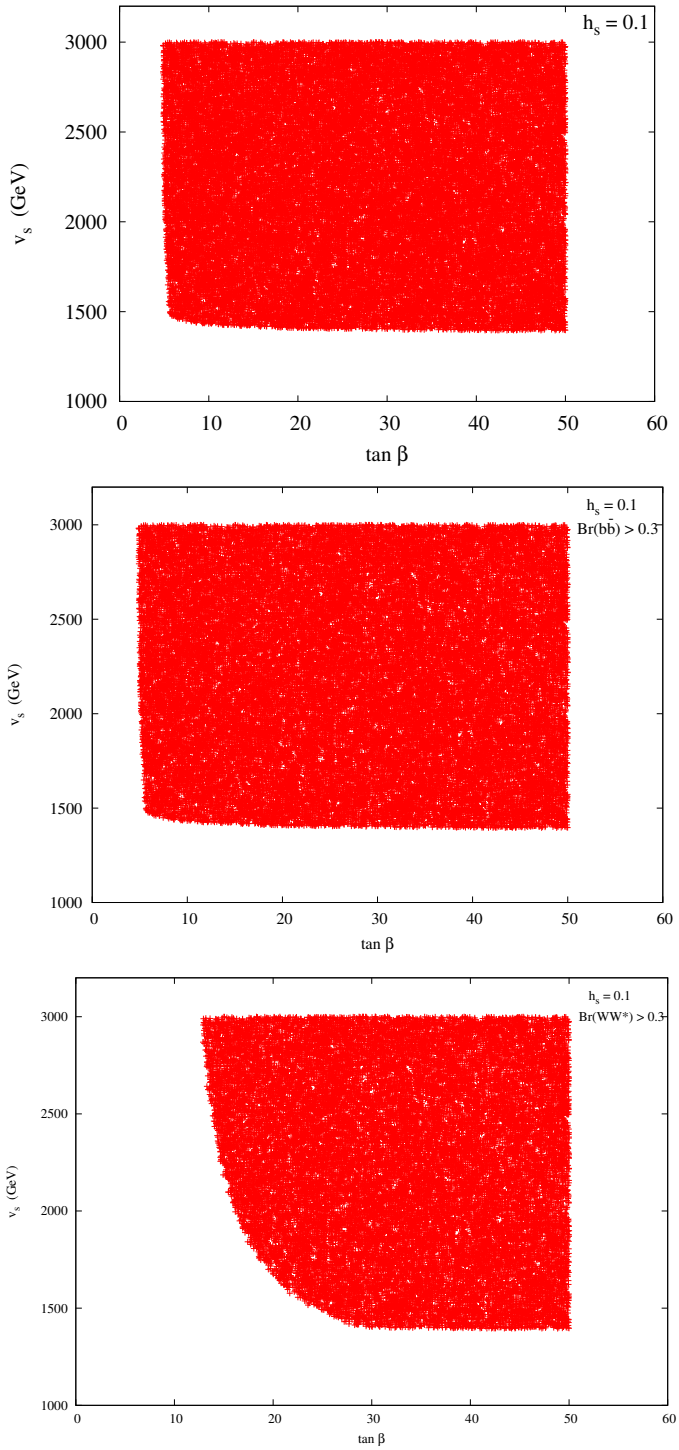

Figure 7. (a) Two-dimensional scatter plots for the parameter-space points satisfying the chargino mass constraint $M_{\tilde{\chi}^{\pm}} > 94\,\text{GeV}$, invisible Z width less than 3 MeV, and $120 < M_{h_{\text{SM-like}}} < 130\,\text{GeV}$, where the SM-like Higgs boson $h_{\text{SM-like}}$ satisfies $O_{k3}^2 < 0.1$ (where $h_k = O_{k1}\phi_d + O_{k2}\phi_u + O_{k3}\phi_s$), (b) also with $B(h_{\text{SM-like}} \to b\bar{b}) > 0.3$, and (c) also with $B(h_{\text{SM-like}} \to WW^*) > 0.3$. Here $h_s = 0.1$.

JHEP06(2012)128

- UMSSM also has a Z' boson at TeV scale.

The SM-like Higgs boson in NMSSM can have nonstandard decays, in contrast to the MSSM. There are two global limits in NMSSM — R symmetry and Pecci-Quinn (PQ) symmetry. In both limits, the lightest CP-odd Higgs boson, a_1, becomes very light after electroweak symmetry breaking. In the R-symmetry limit, the SM-like Higgs boson can decay dominantly into a pair of a_1, which would then significantly affect other decay modes such as diphotons, $b\bar{b}$, WW, and ZZ. If so the production rates into $\gamma\gamma$, WW, ZZ, and $b\bar{b}$ would be substantially smaller than the current data. In this case, the possible detection could be a 4-fermion final state $h \to a_1 a_1 \to f\bar{f}f\bar{f}$.

On the other hand, in the PQ-symmetry limit the h_1 and $\tilde{\chi}_1^0$ are also light. However, the decays of the SM-like Higgs boson into $h_1 h_1$ and $a_1 a_1$ are shown to be suppressed [58]. Similarly, there is also suppression for $h_{\rm SM-like} \to \tilde{\chi}_1^0 \tilde{\chi}_1^0$. In this case, the decay of the SM-like Higgs boson is similar to the usual MSSM Higgs boson. However, if the second lightest neutralino is also light and $M_{h_{\rm SM-like}} > m_{\tilde{\chi}_1^0} + m_{\tilde{\chi}_2^0}$, then $h_{\rm SM-like} \to \tilde{\chi}_1^0 \tilde{\chi}_2^0$ is possible. The $\tilde{\chi}_2^0$ further decays into $\tilde{\chi}_1^0 + h_1$ (or a_1). It would then significantly affect other decay modes such as diphotons, $b\bar{b}$, WW, and ZZ, and therefore the production rates into $\gamma\gamma$, WW, ZZ, and $b\bar{b}$ would be substantially smaller than the current data. The final state for the SM-like boson would then be a pair of fermions plus a large missing energy.

Furthermore, if the SM-like Higgs boson of NMSSM or UMSSM falls into the mass range heavier than 130 GeV, where the current data almost ruled out a SM-like Higgs boson, one has to hide the Higgs boson. In the NMSSM, one can hide it via either the decay into a neutralino pair or into a pair of light pseudoscalar bosons which further decay into light fermions; while in the UMSSM the SM-like Higgs boson can be hidden via decays into the lightest neutralinos. On the other hand, if the SM-like Higgs boson falls in the mass range 120–130 GeV, we have to find regions of parameter space where the SM-like Higgs boson decays into light neutralinos and pseudoscalars have to be suppressed; while in the UMSSM the decay into light neutralinos is to be suppressed.

To recap, the search for the final missing piece of the SM, the Higgs boson, remains a tantalizing task for both experimentalists and theorists. We have demonstrated that in models beyond the SM like the UMSSM, we might be entertained by a SM-like Higgs boson as a mimicker at the LHC. This SM-like Higgs boson can be light in the mass range of 120–130 GeV as indicated by the recent LHC data and behaves almost the same as the SM one or it can decay dominantly into invisible modes and therefore somewhat be hidden if it is heavier. More data are definitely needed at the LHC for detailed studies in order to differentiate among many variants of Higgs bosons once we go beyond the SM.

Acknowledgments

We thank Rong-Shyang Lu for interesting discussion on the ATLAS Higgs searches. This work was supported in parts by the National Science Council of Taiwan under Grant Nos. 99-2112-M-007-005-MY3 and 98-2112-M-001-014-MY3, and the WCU program through the KOSEF funded by the MEST (R31-2008-000-10057-0).

JHEP06(2012)128

References

[1] ATLAS collaboration, A. Nisati, *Higgs searches at ATLAS*, talk given at *XXV International symposium on lepton photon interactions at high energies*, August 22-27, Mumbai, India (2011).

[2] CMS collaboration, V. Sharma, *Higgs searches at CMS*, talk given at *XXV International symposium on lepton photon interactions at high energies*, August 22-27, Mumbai, India (2011).

[3] CMS collaboration, K. Sung, *A search for Higgs boson in* $H \to W^+W^-$, arXiv:1109.2457 [INSPIRE].

[4] ATLAS collaboration, *Combined standard model Higgs boson searches with up to* 2.3 fb^{-1} *of pp collisions at* $\sqrt{s} = 7$ *TeV at the LHC*, ATLAS-CONF-2011-157 (2011).

[5] CMS collaboration, *Combined standard model Higgs boson searches with up to* 2.3 fb^{-1} *of pp collisions at* $\sqrt{s} = 7$ *TeV at the LHC*, CMS-PAS-HIG-11-023 (2011).

[6] ATLAS collaboration, *Combination of higgs boson searches with up to* 4.9 fb^{-1} *of pp collisions data taken at a center-of-mass energy of* 7 *TeV with the ATLAS experiment at the LHC*, ATLAS-CONF-2011-163 (2011).

[7] CMS collaboration, *Combination of SM Higgs searches*, CMS-PAS-HIG-11-032 (2011)

[8] A. Delgado, C. Kolda, A. de la Puente, C. Kolda and A. de la Puente, *Solving the hierarchy problem with a light singlet and supersymmetric mass terms*, *Phys. Lett.* **B 710** (2012) 460 [arXiv:1111.4008] [INSPIRE].

[9] H. Baer, V. Barger, P. Huang and A. Mustafayev, *Implications of a high mass light MSSM Higgs scalar for SUSY searches at the LHC*, *Phys. Rev.* **D 84** (2011) 091701 [arXiv:1109.3197] [INSPIRE].

[10] Y. Huo, T. Li, D.V. Nanopoulos and C. Tong, *The lightest CP-even Higgs boson mass in the testable flipped* $\mathrm{SU}(5) \times \mathrm{U}(1)_X$ *models from F-theory*, arXiv:1109.2329 [INSPIRE].

[11] K. Nakayama, N. Yokozaki and K. Yonekura, *Relaxing the Higgs mass bound in singlet extensions of the MSSM*, *JHEP* **11** (2011) 021 [arXiv:1108.4338] [INSPIRE].

[12] E. Ma, *Exceeding the MSSM Higgs mass bound in a special class of* U(1) *gauge models*, *Phys. Lett.* **B 705** (2011) 320 [arXiv:1108.4029] [INSPIRE].

[13] M. Endo, K. Hamaguchi, S. Iwamoto and N. Yokozaki, *Higgs mass and muon anomalous magnetic moment in supersymmetric models with vector-like matters*, *Phys. Rev.* **D 84** (2011) 075017 [arXiv:1108.3071] [INSPIRE].

[14] M. Asano, T. Moroi, R. Sato and T.T. Yanagida, *Non-anomalous discrete R-symmetry, extra matters and enhancement of the lightest SUSY Higgs mass*, *Phys. Lett.* **B 705** (2011) 337 [arXiv:1108.2402] [INSPIRE].

[15] A. Elsayed, S. Khalil and S. Moretti, *Higgs mass corrections in the SUSY B-L model with inverse seesaw*, arXiv:1106.2130 [INSPIRE].

[16] X.-G. He and J. Tandean, *Hidden Higgs boson at the LHC and light dark matter searches*, *Phys. Rev.* **D 84** (2011) 075018 [arXiv:1109.1277] [INSPIRE].

[17] M. Raidal and A. Strumia, *Hints for a non-standard Higgs boson from the LHC*, *Phys. Rev.* **D 84** (2011) 077701 [arXiv:1108.4903] [INSPIRE].

[18] U. Ellwanger, *Higgs bosons in the next-to-minimal supersymmetric standard model at the LHC*, *Eur. Phys. J.* **C 71** (2011) 1782 [arXiv:1108.0157] [INSPIRE].

JHEP06(2012)128

[19] M. Carena, P. Draper, T. Liu and C. Wagner, *The 7 TeV LHC reach for MSSM Higgs bosons*, *Phys. Rev.* **D 84** (2011) 095010 [arXiv:1107.4354] [INSPIRE].

[20] Y. Mambrini, *Higgs searches and singlet scalar dark matter: combined constraints from XENON 100 and the LHC*, *Phys. Rev.* **D 84** (2011) 115017 [arXiv:1108.0671] [INSPIRE].

[21] E. Ma, *Hiding the Higgs boson from prying eyes*, *Phys. Lett.* **B 706** (2012) 350 [arXiv:1109.4177] [INSPIRE].

[22] I. Low, P. Schwaller, G. Shaughnessy and C.E. Wagner, *The dark side of the Higgs boson*, *Phys. Rev.* **D 85** (2012) 015009 [arXiv:1110.4405] [INSPIRE].

[23] C. Englert, J. Jaeckel, E. Re and M. Spannowsky, *Evasive Higgs maneuvers at the LHC*, *Phys. Rev.* **D 85** (2012) 035008 [arXiv:1111.1719] [INSPIRE].

[24] O. Lebedev, H.M. Lee and Y. Mambrini, *Vector Higgs-portal dark matter and the invisible Higgs*, *Phys. Lett.* **B 707** (2012) 570 [arXiv:1111.4482] [INSPIRE].

[25] R. Foot, A. Kobakhidze and R.R. Volkas, *ATLAS and CMS hints for a mirror Higgs boson*, *Phys. Rev.* **D 84** (2011) 095032 [arXiv:1109.0919] [INSPIRE].

[26] M. Pospelov and A. Ritz, *Higgs decays to dark matter: beyond the minimal model*, *Phys. Rev.* **D 84** (2011) 113001 [arXiv:1109.4872] [INSPIRE].

[27] E. Weihs and J. Zurita, *Dark Higgs models at the 7 TeV LHC*, *JHEP* **02** (2012) 041 [arXiv:1110.5909] [INSPIRE].

[28] J.-W. Cui, H.-J. He, L.-C. Lu and F.-R. Yin, *Spontaneous mirror parity violation, common origin of matter and dark matter and the LHC signatures*, *Phys. Rev.* **D 85** (2012) 096003 [arXiv:1110.6893] [INSPIRE].

[29] B. Bellazzini, C. Csáki, A. Falkowski and A. Weiler, *Buried Higgs*, *Phys. Rev.* **D 80** (2009) 075008 [arXiv:0906.3026] [INSPIRE].

[30] Y. Bai, J. Fan and J.L. Hewett, *Hiding a heavy Higgs boson at the 7 TeV LHC*, arXiv:1112.1964 [INSPIRE].

[31] D. Albornoz Vasquez, G. Bélanger, R. Godbole and A. Pukhov, *The Higgs boson in the MSSM in light of the LHC*, arXiv:1112.2200 [INSPIRE].

[32] B.A. Dobrescu, G.D. Kribs and A. Martin, *Higgs underproduction at the LHC*, *Phys. Rev.* **D 85** (2012) 074031 [arXiv:1112.2208] [INSPIRE].

[33] A. Djouadi, O. Lebedev, Y. Mambrini and J. Quevillon, *Implications of LHC searches for Higgs-portal dark matter*, *Phys. Lett.* **B 709** (2012) 65 [arXiv:1112.3299] [INSPIRE].

[34] C. Englert, T. Plehn, D. Zerwas and P.M. Zerwas, *Exploring the Higgs portal*, *Phys. Lett.* **B 703** (2011) 298 [arXiv:1106.3097] [INSPIRE].

[35] S.-W. Baek, P. Ko and W.-I. Park, *Search for the Higgs portal to a singlet fermionic dark matter at the LHC*, *JHEP* **02** (2012) 047 [arXiv:1112.1847] [INSPIRE].

[36] B. Batell, S. Gori and L.-T. Wang, *Exploring the Higgs portal with* $10\,fb^{-1}$ *at the LHC*, arXiv:1112.5180 [INSPIRE].

[37] H. Baer, V. Barger and A. Mustafayev, *Implications of a 125 GeV Higgs scalar for LHC SUSY and neutralino dark matter searches*, *Phys. Rev.* **D 85** (2012) 075010 [arXiv:1112.3017] [INSPIRE].

[38] S. Heinemeyer, O. Stal and G. Weiglein, *Interpreting the LHC Higgs search results in the MSSM*, *Phys. Lett.* **B 710** (2012) 201 [arXiv:1112.3026] [INSPIRE].

JHEP06(2012)128

[39] A. Arbey, M. Battaglia, A. Djouadi, F. Mahmoudi and J. Quevillon, *Implications of a* 125 *GeV Higgs for supersymmetric models*, *Phys. Lett.* **B 708** (2012) 162 [arXiv:1112.3028] [INSPIRE].

[40] P. Draper, P. Meade, M. Reece and D. Shih, *Implications of a* 125 *GeV Higgs for the MSSM and low-scale SUSY breaking*, *Phys. Rev.* **D 85** (2012) 095007 [arXiv:1112.3068] [INSPIRE].

[41] M. Carena, S. Gori, N.R. Shah and C.E. Wagner, *A* 125 *GeV SM-like Higgs in the MSSM and the* $\gamma\gamma$ *rate*, *JHEP* **03** (2012) 014 [arXiv:1112.3336] [INSPIRE].

[42] S. Akula, B. Altunkaynak, D. Feldman, P. Nath and G. Peim, *Higgs boson mass predictions in SUGRA unification, recent LHC-7 results and dark matter*, *Phys. Rev.* **D 85** (2012) 075001 [arXiv:1112.3645] [INSPIRE].

[43] M. Kadastik, K. Kannike, A. Racioppi and M. Raidal, *Implications of the* 125 *GeV Higgs boson for scalar dark matter and for the CMSSM phenomenology*, *JHEP* **05** (2012) 061 [arXiv:1112.3647] [INSPIRE].

[44] J. Cao, Z. Heng, D. Li and J.M. Yang, *Current experimental constraints on the lightest Higgs boson mass in the constrained MSSM*, *Phys. Lett.* **B 710** (2012) 665 [arXiv:1112.4391] [INSPIRE].

[45] K. Cheung and T.-C. Yuan, *Could the excess seen at* 124–126 *GeV be due to the Randall-Sundrum radion?*, *Phys. Rev. Lett.* **108** (2012) 141602 [arXiv:1112.4146] [INSPIRE].

[46] F. Goertz, U. Haisch and M. Neubert, *Bounds on warped extra dimensions from a standard model-like Higgs boson*, *Phys. Lett.* **B 713** (2012) 23 [arXiv:1112.5099] [INSPIRE].

[47] A. Arhrib, R. Benbrik and N. Gaur, $H \to \gamma\gamma$ *in inert Higgs doublet model*, *Phys. Rev.* **D 85** (2012) 095021 [arXiv:1201.2644] [INSPIRE].

[48] D. Choudhury and P. Saha, *Higgs production as a probe of anomalous top couplings*, arXiv:1201.4130 [INSPIRE].

[49] A. Arhrib, R. Benbrik, M. Chabab, G. Moultaka and L. Rahili, *Higgs boson decay into* 2 *photons in the type II seesaw model*, *JHEP* **04** (2012) 136 [arXiv:1112.5453] [INSPIRE].

[50] U. Ellwanger, C. Hugonie and A.M. Teixeira, *The next-to-minimal supersymmetric standard model*, *Phys. Rept.* **496** (2010) 1 [arXiv:0910.1785] [INSPIRE].

[51] P. Langacker, *The physics of heavy* Z' *gauge bosons*, *Rev. Mod. Phys.* **81** (2009) 1199 [arXiv:0801.1345] [INSPIRE].

[52] C.-F. Chang, K. Cheung and T.-C. Yuan, *Supersymmetric decays of the* Z' *boson*, *JHEP* **09** (2011) 058 [arXiv:1107.1133] [INSPIRE].

[53] J. Kang and P. Langacker, Z' *discovery limits for supersymmetric* E_6 *models*, *Phys. Rev.* **D 71** (2005) 035014 [hep-ph/0412190] [INSPIRE].

[54] R. Dermisek and J.F. Gunion, *The NMSSM close to the R-symmetry limit and naturalness in* $h \to aa$ *decays for* $m_a < 2m_b$, *Phys. Rev.* **D 75** (2007) 075019 [hep-ph/0611142] [INSPIRE].

[55] J.F. Gunion, Y. Jiang and S. Kraml, *The constrained NMSSM and Higgs near* 125 *GeV*, *Phys. Lett.* **B 710** (2012) 454 [arXiv:1201.0982] [INSPIRE].

[56] U. Ellwanger, *A Higgs boson near* 125 *GeV with enhanced di-photon signal in the NMSSM*, *JHEP* **03** (2012) 044 [arXiv:1112.3548] [INSPIRE].

[57] S. King, M. Muhlleitner and R. Nevzorov, *NMSSM Higgs benchmarks near* 125 *GeV*, *Nucl. Phys.* **B 860** (2012) 207 [arXiv:1201.2671] [INSPIRE].

JHEP06(2012)128

[58] P. Draper, T. Liu, C.E. Wagner, L.-T. Wang and H. Zhang, *Dark light Higgs*, *Phys. Rev. Lett.* **106** (2011) 121805 [arXiv:1009.3963] [INSPIRE].

[59] V. Barger, P. Langacker and H.-S. Lee, *Lightest neutralino in extensions of the MSSM*, *Phys. Lett.* **B 630** (2005) 85 [hep-ph/0508027] [INSPIRE].

[60] V. Barger, P. Langacker and G. Shaughnessy, *Neutralino signatures of the singlet extended MSSM*, *Phys. Lett.* **B 644** (2007) 361 [hep-ph/0609068] [INSPIRE].

[61] V. Barger, P. Langacker and G. Shaughnessy, *Collider signatures of singlet extended Higgs sectors*, *Phys. Rev.* **D 75** (2007) 055013 [hep-ph/0611239] [INSPIRE].

[62] V. Barger, P. Langacker, H.-S. Lee and G. Shaughnessy, *Higgs sector in extensions of the MSSM*, *Phys. Rev.* **D 73** (2006) 115010 [hep-ph/0603247] [INSPIRE].

[63] S. Choi, H. Haber, J. Kalinowski and P. Zerwas, *The neutralino sector in the* U(1)*-extended supersymmetric standard model*, *Nucl. Phys.* **B 778** (2007) 85 [hep-ph/0612218] [INSPIRE].

[64] ATLAS collaboration, G. Aad et al., *Search for high mass dilepton resonances in pp collisions at* $\sqrt{s} = 7$ *TeV with the ATLAS experiment*, *Phys. Lett.* **B 700** (2011) 163 [arXiv:1103.6218] [INSPIRE].

[65] ATLAS collaboration, G. Aad et al., *Search for dilepton resonances in pp collisions at* $\sqrt{s} = 7$ *TeV with the ATLAS detector*, *Phys. Rev. Lett.* **107** (2011) 272002 [arXiv:1108.1582] [INSPIRE].

[66] Particle Data Group collaboration, K. Nakamura et al., *Review of particle physics*, *J. Phys.* **G 37** (2010) 075021 [INSPIRE].

JHEP06(2012)128